The T3SS structural and effector genes of *Chlamydia trachomatis* are expressed in distinct phenotypic cell forms.

Authors:
Nicole A. Grieshaber, Cody Appa, Megan Ward, Alorah Grossman, Sean McCormik, Brendan S. Grieshaber, Travis Chiarelli, Hong Yang, Anders Omsland, and Scott S. Grieshaber

Abstract:
Bacteria in the chlamydiales order are obligate intracellular parasites of eukaryotic cells. Within this order, the genus *Chlamydia* contains the causative agents of a number of clinically important infections of humans. Biovars of *C. trachomatis* are the causative agents of trachoma, the leading cause of preventable blindness worldwide, as well as sexually transmitted infections with the potential to cause pelvic inflammatory disease and infertility. Irrespective of the resulting disease, all chlamydial species share the same obligate intracellular life cycle and developmental cell forms. They are reliant on an infectious cycle consisting of at least three phenotypically distinct cell forms termed the reticulate body (RB), the intermediate body (IB) and the elementary body (EB). The EB is infectious but does not replicate. The RB replicates in the host cell but is non-infectious, while the IB is an intermediate form that transitions to the EB form. In this study, we ectopically expressed the transcriptional repressor Euo, the two nucleoid-associated proteins HctA and HctB, and the two component sensor kinase CtcB in the RB. Transcriptional analysis using RNA-seq, differential expression clustering and fluorescence *in situ* hybridization analysis show that the chlamydial developmental cycle is driven by three distinct regulons corresponding to the RB, IB or EB cell forms. Moreover, we show that the genes for the T3SS were cell type restricted, suggesting defined functional roles for the T3SS in specific cell forms.

Importance:
Chlamydia trachomatis, a sexually transmitted bacterial infection, poses a significant global health threat, causing over 100 million infections annually and leading to complications like ectopic pregnancy and infertility. This study investigates the gene expression patterns of *Chlamydia trachomatis* during its unique life cycle within human cells. As an obligate intracellular parasite, *C. trachomatis* transitions through distinct developmental stages - one for infection and dissemination, another for replication, and a third for transitioning back to the infectious form. By analyzing gene expression profiles at each stage, we identified key genes involved in these processes. Interestingly, our research also reveals the presence of two separate T3SS (Type III Secretion System) translocons expressed in distinct stages, suggesting their crucial roles in specific functions during the infection cycle.

Introduction:

Many bacterial species undergo dramatic phenotypic changes to adapt to different environments or to generate cells with specific physiological functions. All the bacteria in the Chlamydiales order are obligate intracellular parasites of eukaryotic cells that undergo a developmental cycle with both non-replicating and actively replicating cell forms [1,2]. Chlamydial species are important pathogens of humans. *C. psittaci* causes zoonotic infections resulting in pneumonia, while *C. pneumoniae* is a human pathogen that causes respiratory disease. Biovars of *C. trachomatis (Ctr)* are the causative agents of trachoma, the leading cause of preventable blindness worldwide, as well as sexually transmitted infections with the potential to cause pelvic inflammatory disease, ectopic pregnancy and infertility [3–5].

The non replicating cell form of *Chlamydia*, the Elementary Body (EB), has reduced metabolic activity but functions in attachment and pathogen-driven infection of eukaryotic host cells [6]. In contrast, the Reticulate Body (RB) is metabolically active and replicative, but cannot infect host cells. Additionally, the chlamydial developmental cycle also generates a third cell type, the Intermediate Body (IB) that is a transitional form that eventually becomes a new EB [7,8]. Transition between cell forms is critical to production of infectious progeny, however the mechanisms that govern these transitions are poorly understood.

Here we investigated the effects of the ectopic expression of four transcriptional regulatory proteins in *Chlamydia trachomatis* (*Ctr*): Euo, HctA, HctB and CtcB. Euo (Early Upstream ORF) is among the earliest genes expressed post EB to RB germination during chlamydial infection [9]. Current evidence suggests that Euo is a DNA binding protein that acts to repress a handful of late cycle genes [9,10]. The HctA protein is a small DNA binding protein that is expressed transiently in the IB cell type ~8-10 hrs, before HctB [7,8]. HctA has been shown to bind DNA and to repress transcription broadly across chromosomes of both *Ctr* and, when ectopically expressed, *E. coli* [11–13]. HctB is a second small positively charged protein that has limited homology to the H1 histone family and is thought to contribute to condensation of the EB nucleoid [14]. Our data show that unlike HctA, HctB is expressed late in EB development, during the final stages of EB formation [7,8]. In addition to these DNA binding proteins, *Ctr* contains a single cytosolic two component regulatory system (TCS) consisting of CtcB/CtcC (histidine kinase/response regulator) [15]. The *Ctr* TCS is actively transcribed during RB to EB development, and the protein products are functional with respect to phosphotransfer [15]. Additionally, expression of the ATPase effector domain of the response regulator, CtcC, resulted in the up regulation of the sigma54 regulon [16]. Using RNA-seq we determined the effects of ectopic expression of these regulatory factors on the transcriptome of *Ctr*, producing gene regulation profiles consistent with cell form-specific transcriptomes. This allowed us to bin the expression of a large fraction of the chlamydial genome into RB, IB and EB-specific transcript categories. We then, using fluorescence *in situ* hybridization fluorescence *in situ* hybridization (FISH), verified that many components of the cell T3SS were expressed in specific cell forms.

Results:

Ectopic expression of Euo, HctA, CtcB, and HctB resulted in arrest of the developmental cycle. Our vectors for ectopic expression of specific proteins in *Ctr* consist of the chlamydial native plasmid, the T5 promoter (sigma70 constitutive promoter) and the E riboswitch for translational conditional expression controlled by the inducer, theophylline (Tph) [17]. The ORFs of each of the four transcriptional regulatory proteins (*euo*, *hctA*, *ctcB*, and *hctB*) were cloned into this plasmid upstream of a C-terminal FLAG tag and transformed into *Chlamydia trachomatis* serovar L2 434/bu (*Ctr*) creating the strains L2-E-euo-FLAG, L2-E-hctA-FLAG, and L2-E-ctcB-FLAG. As described previously, we could not successfully transform *Ctr* with the E-hctB-FLAG construct, therefore we developed a tet-riboJ-E promoter system that combines both transcriptional and translational control to hctB-FLAG expression, creating the strain L2-tet-J-E-hctB-FLAG [17]. Cos-7 cells were infected with each strain and expression of Euo-FLAG, HctA-FLAG and CtcB-FLAG was induced with 0.5 mM Tph at 15 hpi. Expression of HctB-FLAG was induced at 15 hpi with 0.5 mM Tph + 30ng/ml anhydrotetracycline (aTc). We tested for the production of infectious progeny (EBs) using a reinfection assay at 48 hpi. Ectopic

expression of all four transcriptional regulatory proteins resulted in a significant inhibition of EB production as compared to the Clover-FLAG controls (Fig 1A). In addition, infected cells were imaged using transmission electron microscopy (TEM). Cells were infected with L2-E-euo-FLAG, L2-E-hctA-FLAG, L2-E-ctcB-FLAG, L2-tet-J-E-hctB-FLAG and L2-E-clover-FLAG, induced for expression at 15 hpi and fixed and prepared for TEM analysis at 30 hpi (Fig 1B). The induced and uninduced Clover-FLAG control samples were indistinguishable . Cells ectopically expressing Euo had inclusions with very few visible EBs and most cells appeared RB like. In the HctB and HctA expressing bacteria, the inclusions contained large aberrant forms as well as cells with dense structures resembling condensed nucleoids. The inclusions of the CtcB expressing bacteria contained both RB and EB-like cells and an increase in intermediate forms, i.e. large cells with condensed nucleoids (Fig 1B). These data suggested that ectopic expression of all transcriptional regulatory proteins resulted in an aborted developmental cycle as indicated by the IFU studies. The underlying mechanisms, as inferred from bacterial ultrastructure, are different and protein dependent.

RNA-seq of the arrested chlamydial strains. To better understand the effects of the ectopic expression of each regulatory protein, we used RNA-seq to characterize the corresponding transcriptomes. We infected Cos-7 cells with each strain (L2-E-clover-FLAG, L2-E-euo-FLAG, L2-E-hctA-FLAG L2-E-ctcB-FLAG and L2-tet-J-E-hctB-FLAG), induced expression at 15 hpi and harvested RNA for library construction at 18 hpi and 24 hpi. Chlamydial RNA was used to construct transcript libraries which were sequenced using the Illumina workflow. The reads were aligned using Bowtie2 [18]. The counts from the aligned reads for each construct were compared to the Clover-FLAG induced samples using DESeq2 [19] to generate differential expression data. We compared the transcriptome of each sample in triplicate using principal component analysis (PCA) and determined that each ectopically expressing strain produced a distinct gene expression pattern (Fig 2A). We have previously described RNA-seq-based transcriptional profiles for *Ctr* [6]. Here, we used the differential gene expression data from 18 hpi vs 24 hpi [6] along with the differential expression data obtained from the ectopic expression experiments to generate hierarchically-clustered heatmaps using python and Seaborn [20] (Fig 2B and C). We used the 24 hpi experiment for Euo and HctB and the 18 hpi experiment for HctA and CtcB as these timepoints showed the largest differences when compared to the Clover induced control. Clustering produced two dominant groups (Fig 2B and C). Both groups featured genes that were dramatically up-regulated between 18 hpi vs 24 hpi during a normal infection (Fig 2B and C, HeLa_24h) suggesting that all of these genes would be considered mid cycle and late genes [21–23]. The major difference between the two cluster groups is the changes in gene expression induced by HctA and CtcB ectopic expression (Fig 2B and C). One of the clusters featured genes that were not dramatically induced upon HctA-FLAG or CtcB-FLAG ectopic expression (Fig 2B). The other cluster showed the opposite with all the genes upregulated by the ectopic expression of HctA-FLAG or CtcB-FLAG (Fig 2C). Ectopic expression of Euo-FLAG and HctB-FLAG led to a down-regulation of both of these sets of genes as compared to the Clover control (Fig 2B and C). Many of the genes in the first cluster (Fig 2B) have been shown to be expressed mid-cycle [22], while a subset of genes in the second cluster (Fig 2A) have been identified to be expressed late in the developmental cycle [22,23]. Additionally, some of the second cluster genes have been identified as sigma54/ctcB-ctcC regulated genes [16].

Gene expression cluster groups map to cell type specific gene expression profiles. Based on our previous published observations [7,8] we reasoned that the chlamydial developmental cycle should be viewed from the perspective of the cell type rather than simply be defined as a timeline of the infection. Accordingly, the developmental cycle could be divided into three major phases; RB amplification, IB production and EB maturation [7,8]. This developmental model produces inclusions that contain all three cell types (RB, IB and EB) as early as 18 hpi. The inclusions continue to contain all three cell types at different ratios until cell lysis or inclusion extrusion. We have previously demonstrated that the promoter for *euo* (*euo*prom) is active in RB

cells, the *hctA* promoter (*hctA*prom) is active in IB cells and the promoter for *hctB* (*hctB*prom) is active in the late IB/EB cells [7,8].

The cell type expression pattern observed for *euo*, *hctA* and *hctB* suggests that the cluster observations can be used to bin gene expression for specific cell types thus generating a list of potential RB, IB and EB expressed genes. Using the clustering data observations, we created a selection criteria to categorize the RNA-seq data into these three categories. Genes for which we observed little to no change after Euo ectopic expression when compared to the Clover control and had little-to-no change between 18 hpi and 24 hpi during a wt infection were designated as RB expressed genes. We designated genes as IB expressed if expression increased from 18 hpi to 24 hpi and were not induced by HctA, CtcB or Euo ectopic expression. Genes were designated as EB expressed if expression was increased from 18 hpi to 24 hpi in the wt infection and were induced by CtcB and HctA ectopic expression but not increased by Euo ectopic expression (Table S1).

We next used volcano plots to visualize the individual effects of each of the ectopic expression constructs on changes in gene expression of all *Ctr* genes. The expression changes were plotted (log2 fold change) vs statistical significance (-log of the p value) and the RB, IB and EB genes designated in Table S1 were highlighted (Fig 3). We plotted changes in gene expression from 18 hpi to 24 hpi from a wt infection, which as expected indicated that the genes from Table S1 designated as RB genes were largely unchanged in gene expression between 18 hpi and 24 hpi, while both the designated IB and EB genes showed increased expression. RB gene expression was for the most part unchanged when Euo was ectopically expressed in contrast to dramatic reductions in the expression of both IB and EB genes (Fig 3, Euo 24hpi vs Clover 24hpi). Both HctA and CtcB ectopic expression dramatically increased the expression of EB genes (Fig 3, HctA and CtcB 18hpi vs Clover 18hpi). HctB ectopic expression also resulted in a dramatic repression in the expression of both IB and EB genes while also increasing the relative expression of a subset of RB genes relative to Clover (Fig 3, HctB 24hpi vs Clover 24hpiE). We noticed that many of the genes that showed increased expression when HctB was ectopically expressed were ribosomal protein genes (Fig 3, Euo 24hpi vs Clover 24hpi).

Fluorescence *in situ* hybridization verification of cell type gene expression. To determine the association of binned genes with specific cell forms we used fluorescence *in situ* hybridization (FISH) to visualize gene expression in cells expressing GFP and RFP from developmental stage-specific promoters. To this end, we constructed two dual promoter reporter constructs to delineate gene expression from the *euo*, *hctA* and *hctB* promoters which we have shown to be associated with RB, IB and EB cells forms respectively. We generated the strains L2-*hctB*prom_Scarlet-*euo*prom_neongreen (L2-BsciEng) and L2-*hctA*prom_Scarlet-*euo*prom_neongreen (L2-AsciEng) which express the RFP mScarlet-I from either the *hctB* promoter or *hctA* promoter along with the GFP protein neongreen driven by *euo* promoter. To validate our system, the mRNA expression of *euo*, *hctA* and *hctB* was visualized in each strain using custom FISH probes from Molecular Instruments (Fig 4). Cos-7 cells were infected with L2-AsciEng and L2-BsciEng and processed for each FISH probe at 24 hpi. Although dual promoter strains were used in these experiments, the data is presented in a single promoter format to simplify presentation. *Euo* and *hctA* data was processed from L2-AsiEng samples and *hctB* data was processed from L2-BsciEng samples. As expected, *euo* mRNA was observed primarily in the *euo*prom+ (RB) cells and not in either of the *hctA*prom+ (IB) or *hctB*prom+ (EB) cells (Fig 4A). The *hctA* mRNA was observed in a subset of cells that had overlap with the *hctA*prom signal but not *euo*prom or *hctB*prom signal (Fig 4B). The *hctB* mRNA was observed in a subset of cells with overlap with *hctA*prom+ and *hctB*prom+ cells but not *euo*pro+ cells (Fig 4C).

To quantify the FISH results, we used the TrackMate plugin in Fiji [24] to identify and measure both the mRNA signal and promoter reporter signal for each chlamydial cell in five inclusions from each infection. Cells were identified by their promoter reporter signal (green) and separately by their mRNA fluorescence signal (pink). The fluorescence intensity was measured and plotted for both channels (FISH and promoter reporter) in

both identified populations. Therefore, each plot represents two identified cell populations per reporter, mRNA+ (pink) population and their corresponding promoter reporter fluorescence intensity, and the promoter reporter+ (green) population and their corresponding FISH signal. This analysis was performed for all three promoter reporters (*euo*p, *hctA*p and *hctB*p) for each FISH mRNA probe (*euo*, *hctA*, and *hctB*) (Fig 4).

RB: *euo* FISH. Using Fiji and TrackMate, we identified individual chlamydial cells expressing the *euo* mRNA in host cells that were infected with the promoter reporter strains expressing fluorescent proteins from the *euo*prom, *hctA*prom, and *hctB*prom. The analysis indicates that the *euo* mRNA+ cell population (pink) when plotted for *euo*prom fluorescence and *euo* mRNA fluorescence were primarily double positive with high levels of both *euo* FISH signal and *euoprom* signal. These *euo* mRNA+ cells from *hctAprom* infections were primarily single positive. This was also observed for the *hctB*prom infections; the *euo* mRNA+ cells when plotted for *euo* mRNA FISH signal intensity against *hctB*prom signal intensity were primarily single positive (Fig 4A).

We also used TrackMate to identify the promoter reporter positive cell populations (green) and plotted the expression intensities of the promoter reporter signals against the *euo* mRNA FISH signal. The *euo*prom+ cells were predominantly double positive (high *euo* mRNA signal, high *euo*prom signal), while the *hctA*prom+ cells and *hctB*prom+ cell populations (green) were predominantly single positive (low *euo* mRNA signal high *hctA*prom or *hctB*prom signal) (Fig 4A).

IB: *hctA* FISH. The *hctA* mRNA positive population was identified in the *euo*prom, *hctA*prom and *hctB*prom infected cells using TrackMate (pink) and the intensities of the *hctA* mRNA FISH signal was plotted against each of the promoter reporter intensity signals. The *hctA* mRNA+ cells from the *euo*prom infection were mostly single positive but had carryover GFP signal from RB *euo*prom expression (Fig 4B). The *hctA* mRNA+ cell population (pink) was mostly double positive when compared to the *hctA*prom signal. Additionally the *hctA* mRNA+ population had little to no *hctB*prom signal (Fig 4B).

Again we identified the promoter reporter positive chlamydial cells (green) and plotted both the promoter reporter signals and the FISH signal. The expression pattern followed a similar pattern. The *euo*prom+ cell population (green) was mostly single positive with a small population of double positive cells presumably from the long lived GFP protein carry-over (Fig 4B). The *hctA*prom+ cell population (green) demonstrated a large double positive sub-population as well as a single positive sub-population that again was likely due to the long half-life of the mScarlet-I protein carried over into the EB population (Fig 4B). The *hctB*prom+ cell population was almost entirely single positive with little *hctA* mRNA signal (Fig 4B).

EB: *hctB* FISH. We performed the same analysis for the *hctB* mRNA+ cells (pink). The *hctB* mRNA+ chlamydial cells were mostly single positive when compared to the *euo*prom signal with some detected long-lived *euo*prom signal (Fig 4C). The *hctB* mRNA+ cells were generally double positive for the *hctA*prom signal and double positive for the *hctB*prom signal (Fig 4C).

For the promoter reporter cells (green), the *euo*prom+ cells had a significant single positive population and a smaller double positive sub-population, while the *hctA*prom+ cells were both single and double positive for the *hctB* mRNA signal. In the *hctB*prom+ cells there was both a single and double positive population (Fig 4C).

Together, these data indicate that, as expected, *euo* mRNA is expressed in RBs (double positive for *euo*prom signal and *euo* mRNA signal), while *hctA* mRNA is expressed in IBs (*hctA*prom+, *hctA* mRNA+ and *hctB*prom negative) and *hctB* mRNA is expressed in late IB/EBs (*hctB*prom+ and *hctB* mRNA+). Therefore, we used this workflow to interrogate cell form gene expression predicted by the RNA-seq clustering, binning and volcano plot analysis.

Validation of *porB* as an IB gene. We next sought to determine if a gene predicted to be expressed in a particular cell form by the RNA-seq clustering experiment could be verified. The porin gene *porB* [25] which clustered with the IB gene group and *hctA*, a proven IB gene, was selected for the analysis. Cells were infected with either L2-AsciEng or L2-BsciEng, fixed at 24 hpi and probed for the *porB* mRNA. Confocal images were

taken and viewed as z projections (Fig 5A). The *porB* mRNA signal (pink) did not completely overlap with the *euo*prom signal (green) and appeared to be expressed in a subset of cells (Fig 5A). The *porB* mRNA had significant but not complete overlap with the *hctA*prom+ cells (green) and almost no overlap with the *hctB*prom+ cells (Fig 4A). Using the TrackMate protocol described above we identified the promoter reporter expressing populations (*euo*prom, *hctA*prom, and *hctB*prom) and then separately, the *porB* mRNA+ population and measured the fluorescence intensity of each channel (fluorescent reporter proteins and mRNA signal within each population). The *porB* mRNA+ population (pink) in the *euo*prom channel experiment were a mix of single and double positive cells. This was also true for the *euo*prom+ population (green). In comparison the *porB* mRNA+ population (pink) in the *hctA*prom channel experiment were primarily double positive, i.e. high *porB* mRNA and high *hctA*prom activity. However, the *hctA*prom+ population (green) was a mix of single positive and double positive cells (Fig 5A). In the *hctB*prom channel experiment the *porB* mRNA signal+ population (pink) were primarily single positive and did not have appreciable *hctB*prom fluorescence. Conversely the *hctB*prom+ population (green) was primarily single positive with low *porB* mRNA signal. Taken together, the *porB* mRNA expression pattern was reminiscent of the *hctA* mRNA expression pattern.

We also evaluated the kinetics of the activity of the *porB* promoter. The *hctA* promoter from AsciEng was replaced with the promoter region of *porB* (-137bp to +30bp) and transformed into *Ctr* to create L2-PsciEng. We used live cell imaging to measure the expression of neongreen driven by *euo*prom and mScarlet-I driven by *porB*prom. Cells were infected with PsciEng at an MOI ~0.3 and imaged for both the neongreen and mScarlet-I fluorescence every 30 minutes from 10 hpi for 55 hours. For comparisons, L2-AsciEng and L2-BsciEng strains were imaged in parallel. As previously published, *euo* promoter activity is detected at ~12 hpi followed by the *hctA* promoter and finally the *hctB* promoters [7,8] (Fig 5B). The kinetics of L2-PsciEng mirrored that of L2-AsciEng. *Euo*prom activity was detected at ~12 hpi followed by the activity of the *porB*prom at ~20 hpi followed by *hctB*prom activity starting at ~26 hpi. Taken together these data suggest that *porB*, as predicted by the RNA-seq clustering experiment, can be considered an IB gene.

Predicted cell type expression of T3SS genes. We noticed an intriguing expression pattern with the type III secretion system (T3SS) structural genes in the clustering data. To explore this observation, we plotted the effects of ectopic expression on the T3SS operons. We used our wt RNA-seq data [6], operon prediction software [26] and the RT-PCR data published by Hefty et. al [27] to annotate the T3SS operons (Table S2) and plotted the expression data using volcano plots. These plots showed that the majority of the T3SS operons were regulated in an IB like pattern; i.e. up-regulated between 18 hpi and 24 hpi, repressed by Euo and HctB ectopic expression, but not induced by CtcB or HctA ectopic expression (Fig 6). The exception to this pattern were the two operons for the T3SS translocons, (*CTL0238, lcrH, copB_2, copD_2*) and (*scc2, CTL0840, copB, copD*). The *CTL0238* operon (*CTL0238*-op) was regulated like an RB gene while the *scc2* operon (*scc2*-op) was regulated like an EB gene (Fig 6).

Cell type expression of T3SS genes by FISH. We next investigated the cell type expression of two of the T3SS operons predicted to be expressed in the IB, the sctL operon and the sctU operon, using custom FISH probes. The sctL operon (*sctL*-op) includes the genes *sctL*, *sctR*, *sctS*, and *sctT* while the sctU operon (*sctU*-op) encodes the genes *sctU*, *sctV*, *lcrD*, *copN*, *scc1*, and *malQ*. Cell monolayers were infected with L2-AsciEng and L2-BsciEng at an moi ~ 0.3 and processed for FISH staining at 24 hpi (Fig 7). FISH signal for both mRNAs (*sctU*-op and *sctL*-op) was observed in cells distinct from *euo*prom+ and *hct*Bprom+ cells (Fig 7A and B) Conversely, both T3SS operon mRNAs were detected in a subset of the *hctA*prom+ cell population. To quantitate this data, we used the TrackMate plugin in FIJI to identify the individual chlamydial cells in 3D z stacks of confocal images of 5 FISH stained inclusions. Again, the fluorescence intensity for both signals in the mRNA positive population (pink) and the promoter reporter population (green) was determined. These data were then plotted to visualize the relative signal for these reporters (Fig 7). For both the *sctL*-op and the

sctU-op the mRNA+ population (pink) plotted for *euo*prom and FISH signal, there was a single positive population (high mRNA signal and low *euo*prom signal) and a double positive population (high mRNA signal and high *euo*prom signal). The *euo*prom+ population (green) were also both single and double positive for both operon FISH signals and *euo*prom signal (Fig 7A and B., *euo*p). For the *hctA*prom reporter, again both the *sctL*-op and *sctU*-op mRNA+ cells (pink) had both single positive and double populations, while the *hctA*prom+ population (green) were also both single and double positive (Fig 7A and B., *hctA*p). In contrast, the mRNA of both the *sctL*-op and the *sctU*-op and *hct*Bprom reporter were distinct single positive populations in the *hctB*prom infections (Fig 7A and B., *hctB*p). This overall expression pattern was very similar to that of the *hctA* mRNA and *porB* mRNA FISH, supporting an IB like gene expression pattern.

As these data suggested that the two operons were expressed in IBs but not RBs, we probed for mRNA expression in L2-AsiEng infections at 16 hpi. At this time point there are few if any IBs present and the vast majority of the chlamydial cells are RBs [8]. As controls, 16 hpi samples were also probed for *hctA* mRNA and *euo* mRNA. As expected, *hctA* mRNA signal was undetectable while *euo* mRNA signal was high. The mRNA signal for *sctL*-op and *sctU*-op was undetectable, which again indicates that these two operons are expressed in the IB cell type and not in RBs (Fig S1).

Cell type expression of the T3SS translocon genes by FISH. As mentioned above, the *Ctr* genome encodes two operons for the T3SS translocon each of which contain four genes, the *CTL0238*-op and the *scc2*-op [28]. This duplication is conserved in all of the vertebrate infecting chlamydial species. The expression profiles from our clustering data and volcano plots suggests that the two translocon operons are expressed in different cell types; the *CTL0238*-op in RBs and the *scc2*-op in EBs (Fig 6). To verify differential cell type expression, L2-BsciEng samples processed at 24 hpi were probed with custom FISH probes designed against C*TL0238*-op and *scc2*-op and imaged by confocal microscopy.

The confocal micrographs showed that the mRNA FISH signal for *CTL0238*-op heavily overlapped with the *euo*prom channel but was distinct from *hctB*prom+ cells (Fig 8,*CTL0238*-op mRNA). In contrast, the mRNA signal for the *scc2*-op was distinct from the *euo*prom+ cells but almost completely overlapped the *hctB*prom+ cells (Fig 8, *scc2*-op mRNA).

To highlight the differential expression of *CTL0238*-op mRNA and *scc2*-op mRNA, we infected cells with L2 AsciEng and processed the samples for FISH at 16 hpi when most of the chlamydial cells are RBs. At 16 hpi essentially all the cells were green (*euo*prom+) with little to no red *hctA*prom+ cells. The green *euo*prom+ cells were all positive for the *CTL0238*-op FISH signal (Sup. Fig 3, *CTL0238*-op). In contrast, the *scc2*-op FISH signal was undetectable in *euo*prom+ cells (Sup. Fig 3, *scc2*-op). Taken together this data supports the observation that the two translocon operons are differentially regulated and are expressed in distinct cell types. The *scc2*-op is expressed in late IB/EB cells while the *CTL0238*-op is expressed in RB cells.

Predicted cell type expression of T3SS effectors. In general, T3SS translocons are involved in interacting with host membranes to facilitate the secretion of T3SS effectors into target cells [29]. During infection, *Ctr* secretes effectors into/through two membrane systems, the host cell plasma membrane and, once inside the cell, the inclusion membrane. Additionally, the chlamydial T3SS is known to secrete different kinds of effectors, soluble proteins as well as the integral membrane inclusion (Inc) proteins [30–33]. Using volcano plots we asked how the genes encoding for the soluble effector proteins (Table S3) and Inc proteins (Table S4) were regulated by the ectopic expression of Euo, HctA, HctB and CtcB. The vast majority of the soluble T3SS effector genes were regulated like EB genes; higher in 18-24 hpi and induced by HctA and CtcB ectopic expression, but down regulated by Euo and HctB ectopic expression (Fig 9A). In contrast, most of the *incs* were regulated like RB genes with the exception of only *incM* and *incV,* which were regulated like EB genes (Table S4 and Fig 9B).

Cell type expression of *inc* genes by FISH. The volcano plots suggested that the majority of the *inc* effector genes were expressed in an RB like pattern. However, two *inc* genes (*incV* and *incM)* stood out as potential EB genes. To determine if the putative late *inc*, *incV* was expressed late in RBs or was a bona fide EB gene, we compared mRNA expression of a known RB expressed *inc*, *incD* to *incV* by FISH. Cos-7 cells infected with L2-BsciEng were probed for the expression of *incD* and *incV* at 16 hpi (mostly RBs) and 24 hpi (all three cell forms). Confocal microscopy revealed that, as expected, *incD* was expressed in *euo*prom+ RB cells at both 16 hpi and 24 hpi and not in *hctB*prom+ EBs present at 24 hpi (Fig 10A). Conversely, *incV* mRNA could not be detected at 16 hpi and was expressed exclusively in *hctB*prom+ EBs (Fig 10B). These data support that *incD* is indeed an RB gene and the hypothesis that *incV*, and likely *incM*, is an EB gene.

Discussion:

The chlamydial developmental cycle has traditionally been defined by the timeline of the infection. The infectious EB invades the host cell and begins to germinate into the RB cell form that then begins to divide. The genes involved in this process have been described as the early genes. Sometime after germination and the initiation of replication, ~18 hpi for *Ctr* serovar L2, transitionary forms appear. The gene expression associated with this timeframe is usually considered the chlamydial mid cycle. At ~24 hpi until cell lysis EBs accumulate in the inclusion. Genes upregulated at this time point and forward are considered late genes [21–23]. We have dissected the developmental cycle and developed a model based on cell type transitions [8]. Our model suggests that the developmental cycle is best described by the transitions from one cell type to another. In our model the EB enters the host cell (through the use of premade effectors) and initiates immediate early protein synthesis (germination genes) to begin the germination process. The germination process takes ~ 10 hours to complete. The completion of germination is defined by the first division of the nascent cell resulting in RB cells. At this stage the RBs expand in number through symmetric division, amplifying the infection. Our model suggests the RBs mature during this amplification stage, ultimately dividing asymmetrically to produce the IB cell form. Our model defines the IB cell form as the committed cell to EB formation. The mature RBs at this stage continue to replicate producing one IB and one RB. These IBs never re-enter the cell cycle and instead transition into the infectious EB form which takes ~ 10 hours to complete [8].

In this study, we ectopically expressed four transcriptional regulatory proteins that all blocked the progression of the developmental cycle. The effects of expression of these regulatory proteins using RNA-seq was determined and compared using a clustering algorithm which resulted in three distinct regulation patterns. The first cluster contained genes that were unaffected by the ectopic expression of Euo and were not upregulated between 18 hpi and 24 hpi of a *Ctr* L2 infection. The second cluster consisted of genes whose expression increased from 18 hpi to 24 hpi of a wt infection and were not induced by ectopic expression of HctA or CtcB. The third cluster of genes were upregulated between 18 hpi and 24 hpi and by the ectopic expression of both HctA and CtcB. These groups fit well into the major cell categories in our model; RBs, IBs and EBs. Using the clustering observation we created selection criteria based on changes in gene expression from our RNA-seq experiments. We were able to bin 639 out of 902 genes into one of the RB, EB, and IB categories. The genes that could not be assigned were either expressed at levels too low to have confidence in the expression pattern or had an unique expression pattern that did not fit into the three categories, suggesting potential unique roles in chlamydial biology.

The RB cell is the replicating cell form leading to expansion of cell numbers. Based on the changes in gene expression after ectopic expression of Euo, HctA, CtcB and HctB we found that 532 genes were regulated as RB genes. Within this category included cell replication genes, genes involved in protein synthesis, genes for many of the Inc proteins and the *euo* gene. Based on our selection criteria this group likely encompasses both potential constitutive genes (expressed in RBs, IBs and potentially early EBs) as well as RB specific genes such as *euo*, *incD* and the *CTL0238*-op which were expressed only in the RB cell form.

The IB cell type is the transitional form between the RB and the EB and is currently poorly defined. We define the IB cell type as the committed step to EB formation; the IB is the cell form that exits the cell cycle and begins the program to transition into the infectious EB [8]. Our data identified 67 genes that are likely expressed in the IB cell type. The functions of these genes vary widely. We identified two porin genes (*porB* and *CLT0626*), two disulfide isomerases (*CTL0149* and *CTL0152*) and six polymorphic outer membrane proteins (*pmpB*, *C, E*, *F*, *G*, and *H*) as IB genes suggesting dramatic changes to the outer membrane of the IB as it transitions into the EB.

The EB cell is the infectious cell form that is "terminally" differentiated. Once formed in the inclusion the EB maintains an infectious phenotype through active metabolism but has very low levels of gene expression [6]. In this study we define the EB genes as the final gene expression cascade that leads to this differentiated from. Of the 46 EB genes, 18 had been previously shown to be directly regulated by the sigma54 alternative sigma factor and 4 were reported to be sigma28 regulated genes [10,16]. The regulation of the remaining 24 genes is unknown. As both HctA ectopic expression and the ectopic expression of CtcB induce the expression of the EB genes, the EB regulon is likely regulated by a complex shift in gene expression and activation of the sigma54 and sigma28 regulons is a part of this shift.

We tested one of the predicted IB genes, *porB*, and showed that its regulation, both by promoter specific gene expression in chlamydial cells and by its developmental kinetics, matched that of *hctA.* This was further confirmed using FISH to demonstrate cell type gene expression matched that of the IB gene, *hctA*. We have previously published the kinetics of the *euo*, *hctA* and *hctB* promoters and showed that the promoter activities fit into the RB, IB and EB model [4,5]. Here we combined these promoter reporter strains with FISH and demonstrated that the *euo* mRNA was expressed primarily in RBs, that *hctA* mRNA was expressed in IBs, and that *hctB* mRNA was expressed in EBs demonstrating the usefulness of FISH for identifying cell type specific gene expression

Overall, this data supports a model that includes (at least) three dominant cell forms: the RB, the IB and the EB. These cells have dramatically different gene expression profiles and phenotypes. The EB has been well characterized as it is the infectious form, does not replicate and has a dramatically condensed nucleoid. The nucleoid structure is due in part to the binding of the two histone like proteins, HctA and HctB to the chromosome [11,14]. Our data indicates that the construction of the compact nucleoid happens in two distinct and temporally separated steps [7,8]. HctA is expressed as an IB gene and, when ectopically expressed, induces the expression of the EB genes suggesting that HctA expression is an important regulator of the IB to EB transition. HctB on the other hand is expressed as an EB gene and its ectopic expression resulted in the inhibition of the expression of most genes with the exception of the ribosomal protein genes suggesting that HctB's role is to form the final condensed nucleoid and turn off all gene expression with the exception of the ribosomal protein genes. This suggests an intriguing hypothesis that the ribosomal protein genes are potentially free of inhibition and that protein synthesis could be rapidly reinitiated upon EB germination. Together this suggest that the transition from the IB to EB occurs in two steps; 1) HctA chromosomal binding turning off RB and IB genes and allowing EB genes to become expressed, and 2) HctB is expressed late in EB formation creating the final condensed nucleoid that potentially spares the ribosomal genes.

Volcano plots of the effects of ectopic expression of the four regulatory genes support the categorization of most chlamydial genes into the RB, IB and EB categories. We specifically focused on the expression of the T3SS operons and observed that the majority of the operons for the structural components were IB-like in their regulation. This was verified using FISH for both the *sctL* operon (*sctL, sctR, sctS, and sctT*) and the *sctU* operon (*sctU, sctV, lcrD, copN, scc1, and malQ*). While the majority of the T3SS structural operons were expressed as IB genes, the two translocon operons (*CTL0238, lcrH, copB_2, copD_2*) and (s*cc2, CTL0840, copB, copD*) were predicted by clustering and volcano plots to be expressed in RB and EB cells respectively. This prediction was again verified by FISH in the context of dual reporter strains.

The observation that the two translocons were expressed in distinct cell forms (*CTL0238*-op in RBs and *scc2*-op in EBs) prompted us to determine the expression of the T3SS effectors. *Ctr* encodes two classes of effectors, soluble and inclusion membrane embedded proteins (Incs) [31,34,35]. The data from this study showed that the majority of the Inc protein effectors (28 out of 36) were expressed as RB genes while the majority of the soluble T3SS effectors (17 out of 23) were expressed as EB genes and that none of the soluble effectors were expressed as RB genes. This pattern suggests an intriguing hypothesis; the *scc2*-op translocon translocates soluble effectors as the EB contacts host cells and mediates entry events, while the *CTL0238*-op is expressed early during the EB to RB germination process in the nascent inclusion and translocates the transmembrane Inc effectors. Whether this separation is temporal or whether the two translocons are specialized for the translocation of soluble vs. inclusion membrane effectors is currently unknown. Interestingly, although the majority of the Inc proteins were expressed as RB genes there were two Incs that were determined to be expressed in EBs, *incV* and *incM*. In addition to its regulation pattern we also verified that *incV* was an EB gene using FISH. Both IncV and IncM are involved in the establishment of early inclusion functions [36,37]. We hypothesize that these "pre-loaded" Inc proteins are among the first to be secreted from internalized *Ctr* after the *CTL0238*-op is deployed.

Ctr communicates and reprograms the host cell to create and maintain its intracellular replication niche in part through the use of a T3SS. We were surprised that the majority of the T3SS operons for the structural components of the system were expressed as IB genes. This expression pattern along with the cell type specific expression of the translocons (one in the RB and one in the EB) and effectors suggests that the T3SS is constructed, deployed and secretes effectors in a cell type specific manner that is likely a critical component of the complex developmental cycle and host cell reprogramming.

Taken together, these data support an overall model that the chlamydial developmental cycle should be viewed as consisting of discrete phenotypic cell forms that transition from one form to the next to generate the developmental cycle (Fig 11). This process creates an infection with mixed phenotypic forms throughout the infection. The data also suggest that the functional role of each cell type is determined by its gene expression profile creating a cycle that proceeds in a single direction. The EB binds to and enters cells in part through the deployment of soluble effectors and the *scc2*-op translocon expressed during EB development. After entry, germination begins and the RB genes are expressed including the *CTL0238*-op translocon which deploys the Inc proteins for the creation of the inclusion replication niche and the genes required for chlamydial replication leading to RB amplification. After an amplification period, the RB matures into a stem cell-like cell form and begins to produce IBs [5]. The IB synthesizes the T3SS structural components and matures into the EB form over ~8-10 hours. That the IB and not the RB expresses the genes for the construction of the T3SS suggests that the T3SS apparatus that entered on the EB cells remains on the RBs and is diluted with every replication. It is unclear if the secretion system gets partitioned equally or is retained in a subset of RBs. The IB also expresses the histone like DNA binding protein, HctA. Our data suggest that HctA has an important role in shifting gene expression from the IB pattern to the EB genes. This is likely in conjunction with the CtcBC two component regulatory system and the sigma54 alternative sigma factor. The EB genes as previously mentioned include the majority of the soluble T3SS effectors and the *scc2*-op translocon as well as the HctB DNA binding protein. We hypothesize that EB gene expression loads the EB with the invasion-related proteins and HctB shuts down the majority of gene expression creating the dense nucleoid, the final step of EB formation. This prepares the EB for the initiation of the next round of infection (Fig 11). Our data has highlighted three categories of gene expression that define the three major phenotypic cell forms, RB, IB and EB. However, future studies are needed to define the regulatory circuits and DNA elements that create these cell form expression patterns.

Our identification of cell type gene expression of a large percentage of the chlamydial genome will aid the determination of the functions of the many hypothetical genes encoded in the chlamydia genome. Understanding the function of many of these genes has been hampered by the mixed cell environment of the

chlamydial inclusion. Additionally, with the emerging genetic tools available to investigate the functional roles of genes during infection, knowing in which cell type they are expressed will improve the interpretation of the results.

Materials and Methods

Cell Culture

Cell lines were obtained from the American Type Culture Collection. Cos-7 cells (CRL-1651) were grown in RPMI-1640, supplemented with 10% FBS and 10 µg/mL gentamicin (Cellgro). *Chlamydia trachomatis* serovar L2 (LGV Bu434) was grown in Cos-7 cells. Elementary Bodies (EBs) were purified by density gradient (DG) centrifugation essentially as described [38] following 48 h of infection. EBs were stored at -80ºC in Sucrose Phosphate Glutamate (SPG) buffer (10 mM sodium phosphate [8mM K2HPO4, 2mM KH2PO4], 220 mM sucrose, 0.50 mM l-glutamic acid, pH 7.4) until use.

Vector Construction

All constructs used p2TK2-SW2 [39] as the backbone and cloning was performed using the In-fusion HD EcoDry Cloning kit (FisherScientific). Primers and geneblocks (gBlocks) were ordered from Integrated DNA Technologies (IDT) and are noted in Table S5. The construction and characterization of p2TK2-SW2-T5-E-clover-3xFLAG (E-clover), p2TK2-SW2-Tet-J-E-clover-3xFLAG (Tet-JE-clover) and p2TK2-SW2-Tet-J-E-hctB-3xFLAG (Tet-JE-hctB) has been described previously [17].

E-hctA-3xFLAG (E-hctA), E-euo-3xFLAG, (E-euo) and E-ctcB-3xFLAG (E-ctcB),

The *hctA*, *euo* and *ctcB* ORFs were amplified from *Ctr* L2(434) using the primers indicated in Table S5. Each fragment was used to replace Clover in p2TK2-SW2-T5-E-clover-3xFLAG.

*hctB*prom_Scarlet-*euo*prom_neongreen (BsciEng), *hctA*prom_Scarlet-*euo*prom_neongreen (AsciEng) and *porB*prom_Scarlet-*euo*prom_neongreen (PsciEng).

The gBlock mScartlet-I (Table S5) was cloned into BMELVA [8] to replace mKate which created the construct BscieLVA. The degradation tag LVA was then removed from neongreen using the primers indicated to create BsciEng. The *hcA* and *porB* promoters were amplified and used to replace the *hctB* promoter using the primers indicated to create AsciEng and PsciEng respectively.

Chlamydial Transformation and Isolation.

Transformation of Ctr L2 was performed essentially as previously described [7]. Briefly, $1x10^8$ EBs + >2µg DNA/well were used to infect a 6 well plate. Transformants were selected over successive passages with 1U/ml penicillin G or 500µg/ml spectinomycin as appropriate for each plasmid. The new strain was clonally isolated via successive rounds of inclusion isolation (MOI, <1) using a micromanipulator. Clonality of each strain was confirmed by isolating the plasmid, transforming into *E. coli* and sequencing six transformants.

Replating Assay.

Ctr were isolated by scraping the infected monolayer into media and pelleting at 17200 rcfs. The EB pellets were resuspended in RPMI via sonication and seeded onto fresh monolayers in a 96-well microplate in a 2-fold dilution series. Infected plates were incubated for 24 hours prior to fixation with methanol and stained with 4′,6-diamidino-2-phenylindole (DAPI) and *Ctr* MOMP Polyclonal Antibody, FITC (Fishersci). The DAPI stain was used for automated microscope focus and visualization of host-cell nuclei, and the anti-*Ctr* antibody was used to visualize the *Ctr* to identify and count inclusions. Inclusions were imaged using a Nikon Eclipse TE300 inverted microscope utilizing a scopeLED lamp at 470nm and 390nm, and BrightLine band pass emissions filters at 514/30nm and 434/17nm. Image acquisition was performed using an Andor Zyla sCMOS in conjunction with µManager software. Images were analyzed using ImageJ software and custom scripts.

Statistical comparisons between treatments were performed using an ANOVA test followed by Tukey's Honest Significant Difference test.

Transmission Electron Microscopy

For analysis of the structure of *Ctr* upon ectopic protein expression, cell monolayers were infected with the indicated strain at an moi of 0.5 and induced with 0.5mM Theophylline at 15 hpi. Infected cells were released from the plate with Trypsin-EDTA at 30 hpi, rinsed with 1xPBS and the pellet was fixed with EM fixative (2%PFA, 2% Glutaraldehyde, 0.1M Phosphate Buffer, pH 7.2) overnight at 4ºC. Fixed pellets were rinsed and dehydrated before embedding with Spurr's resin and cross sectioned with an ultramicrotome (Riechert Ultracut R; Leica). Ultra-thin sections were placed on formvar coated slot grids and stained with uranyl acetate and Reynolds lead citrate. TEM imaging was conducted with a Tecnai G2 transmission electron microscope (FEI Company; Hillsboro, OR).

RNA-Seq

Total RNA was isolated from cells infected with the indicated strains. Expression of each protein was induced at 15 hpi with either 0.5 mM theophylline and 30ng/ml anhydrotetracycline (HctB) or 0.5 mM theophylline (Clover, HctA, CtcB and Euo) and the *Ctr* isolated at 18 and 24 hpi on ice. Briefly, the infected monolayer was scraped into ice cold PBS, lysed using a Dounce homogenizer and the *Ctr* isolated over a 30% MD-76R pad. Total RNA was isolated using TRIzol reagent (Life Technologies) following the protocol provided and genomic DNA removed (TURBO DNA-free Kit, Invitrogen). The enriched RNA samples were quantified and the libraries built and barcoded by the IBEST Genomics Resources Core at the University of Idaho. The libraries were sequenced by University of Oregon sequencing core using the Illumina NovaSeq platform. RNA-seq reads were aligned to the published *Ctr* L2 Bu 434 genome using the Bowtie2 aligner software [18]. Reads were quantified using HTseq [40]. Statistical analysis and normalization of read counts was accomplished using DESeq2 in R [19]. Log2fold change and statistics were also calculated using DESeq2. Heatmaps and hierarchical clustering were generated and visualized using Python with Pandas and the Seaborn visualization package [6]. Aligned reads are accessible from the NCBI's Gene Expression Omnibus with the accession number of GSE262652. Volcano plots were constructed from the log2fold change data using Python and the Bokeh plotting library (Bokeh Development Team).

RNA fluorescence in situ hybridization (RNA-FISH)

All FISH probes were designed by Molecular Instruments (Los Angeles, CA) using the sequence indicated in (Tabel S6). Cos7 monolayers seeded on coverslips were infected with the indicated strains at an MOI ~ 0.3. Infected cells were fixed at the indicated times in 4% paraformaldehyde (PFA) for 10 min at RT at 24 hpi, washed 2x with 1XPBS and dehydrated overnight at -20ºC in 70% EtOH. Samples were probed and the signal was amplified as described by the protocol provided by Molecular Instruments with the exception that DAPI was added to the final wash to visualize DNA. Coverslips were mounted on a microscope slide with MOWIOL® mounting solution (100 mg/mL MOWIOL® 4-88, 25% glycerol, 0.1 M Tris pH 8.5).

Fluorescence images were acquired using a Nikon spinning disk confocal system with a 60x oil-immersion objective, equipped with an Andor Ixon EMCCD camera, under the control of the Nikon elements software. Images were processed using the image analysis software ImageJ (http://rsb.info.nih.gov/ij/). Representative confocal micrographs displayed in the figures are maximal intensity projections of the 3D data sets, unless otherwise noted.

Live cell imaging

Monolayers of Cos7 cells were grown in a glass bottom 24 well plate and infected with the promoter reporter strains L2-BsciEng, L2-AsciEng and L2-PsciEng. Live cell imaging of the developing inclusions was started at

8 hpi using an automated Nikon epifluorescent microscope equipped with an Okolab (http://www.oko-lab.com/live-cell-imaging) temperature controlled stage and an Andor Zyla sCMOS camera (http://www.andor.com). Multiple fields of view from each well were imaged every fifteen minutes. The fluorescence intensity of each inclusion over time was tracked using the ImageJ plugin TrackMate [24] and the results were averaged and plotted using python and matplotlib [41].

References:

1. Abdelrahman, Y.M., and Belland, R.J. (2005). The chlamydial developmental cycle. FEMS Microbiol. Rev. *29*, 949–959. 10.1016/J.FEMSRE.2005.03.002.
2. Rockey, D.D., and Matsumoto, A. (1996). The chalmydial developmental cycle. In (ASM Press, Washington D. C.), pp. 403–425.
3. Grieshaber, S., Grieshaber, N., Yang, H., Baxter, B., Hackstadt, T., and Omsland, A. (2018). Impact of Active Metabolism on Chlamydia trachomatis Elementary Body Transcript Profile and Infectivity. J. Bacteriol. *200*. 10.1128/JB.00065-18.
4. Chiarelli, T.J., Grieshaber, N.A., Omsland, A., Remien, C.H., and Grieshaber, S.S. (2020). Single-Inclusion Kinetics of Chlamydia trachomatis Development. MSystems *5*. 10.1128/MSYSTEMS.00689-20.
5. Chiarelli, T.J., Grieshaber, N.A., Appa, C.R., and Grieshababer, S.S. (2023). Computational Modeling of the Chlamydial Developmental Cycle Reveals a Potential Role for Asymmetric Division. mSystems *8*, e00053-23. 10.1128/msystems.00053-23.
6. Rosario, C.J., and Tan, M. (2012). The early gene product EUO is a transcriptional repressor that selectively regulates promoters of Chlamydia late genes. Mol. Microbiol. *84*, 1097–1107. 10.1111/J.1365-2958.2012.08077.X.
7. Hakiem, O.R., Rizvi, S.M.A., Ramirez, C., and Tan, M. Euo is a developmental regulator that represses late genes and activates midcycle genes in *Chlamydia trachomatis*. mBio *0*, e00465-23. 10.1128/mbio.00465-23.
8. Barry, C.E., Brickman, T.J., and Hackstadt, T. (1990). Hc1-mediated effects on DNA structure: a potential regulator of chlamydial development. Mol. Microbiol. *9*, 273–283. 10.1111/j.1365-2958.1993.tb01689.x.
9. Grieshaber, N.A., Grieshaber, S.S., Fischer, E.R., and Hackstadt, T. A small RNA inhibits translation of the histone-like protein Hc1 in Chlamydia trachomatis. Mol. Microbiol. *59*, 541–550. 10.1111/j.1365-2958.2005.04949.x.
10. Grieshaber, N.A., Fischer, E.R., Mead, D.J., Dooley, C.A., and Hackstadt, T. Chlamydial histone-DNA interactions are disrupted by a metabolite in the methylerythritol phosphate pathway of isoprenoid biosynthesis. Proc. Natl. Acad. Sci. U. S. A. *101*, 7451–7456. 10.1073/pnas.0400754101.
11. Brickman, T.J., Barry, C.E. 3rd, and Hackstadt, T. (1991). Molecular cloning and expression of hctB encoding a strain-variant chlamydial histone-like protein with DNA-binding activity. J. Bacteriol. *175*.
12. Koo, I.C., and Stephens, R.S. (2003). A developmentally regulated two-component signal transduction system in Chlamydia. J. Biol. Chem. *278*, 17314–17319. 10.1074/JBC.M212170200.
13. Soules, K.R., LaBrie, S.D., May, B.H., and Hefty, P.S. (2020). Sigma 54-Regulated Transcription Is Associated with Membrane Reorganization and Type III Secretion Effectors during Conversion to Infectious Forms of Chlamydia trachomatis. MBio *11*. 10.1128/MBIO.01725-20.
14. Grieshaber, N.A., Chiarelli, T.J., Appa, C.R., Neiswanger, G., Peretti, K., and Grieshaber, S.S. (2022). Translational gene expression control in Chlamydia trachomatis. PLoS ONE *17*. 10.1371/JOURNAL.PONE.0257259.
15. Langmead, B., and Salzberg, S.L. (2012). Fast gapped-read alignment with Bowtie 2. Nat. Methods *9*, 357–359. 10.1038/nmeth.1923.
16. Love, M.I., Huber, W., and Anders, S. (2012). Moderated estimation of fold change and dispersion for RNA-seq data with DESeq2. Genome Biol *15*. 10.1186/s13059-014-0550-8.
17. Nicholson, T.L., Olinger, L., Chong, K., Schoolnik, G., and Stephens, R.S. (2001). Global Stage-Specific Gene Regulation during the Developmental Cycle of Chlamydia trachomatis. J. Bacteriol. *185*, 3179–3189. 10.1128/JB.185.10.3179-3189.2003.
18. Shaw, E.I., Dooley, C.A., Fischer, E.R., Scidmore, M.A., Fields, K.A., and Hackstadt, T. Three temporal classes of gene expression during the Chlamydia trachomatis developmental cycle. Mol. Microbiol. *37*, 913–925.
19. Belland, R.J., Zhong, G., Crane, D.D., Hogan, D., Sturdevant, D., Sharma, J., Beatty, W.L., and Caldwell, H.D. (2003). Genomic transcriptional profiling of the developmental cycle of Chlamydia trachomatis. Proc. Natl. Acad. Sci. *100*, 8478–8483. 10.1073/PNAS.1331135100.
20. Tinevez, J.-Y., Perry, N., Schindelin, J., Hoopes, G.M., Reynolds, G.D., Laplantine, E., Bednarek, S.Y., Shorte, S.L., and Eliceiri, K.W. (2014). TrackMate: An open and extensible platform for single-particle tracking. Methods *115*, 80–90. 10.1016/j.ymeth.2016.09.016.
21. Price, M.N., Huang, K.H., Alm, E.J., and Arkin, A.P. (2005). A novel method for accurate operon predictions

in all sequenced prokaryotes. Nucleic Acids Res. *33*, 880–892. 10.1093/nar/gki232.
22. Hefty, P.S., and Stephens, R.S. (2007). Chlamydial type III secretion system is encoded on ten operons preceded by sigma 70-like promoter elements. J. Bacteriol. *189*, 198–206. 10.1128/JB.01034-06.
23. Stephens, R.S., Kalman, S., Lammel, C., Fan, J., Marathe, R., Aravind, L., Mitchell, W., Olinger, L., Tatusov, R.L., Zhao, Q., et al. (1998). Genome sequence of an obligate intracellular pathogen of humans: Chlamydia trachomatis. Science *282*, 754–759. 10.1126/SCIENCE.282.5389.754.
24. Dey, S., Chakravarty, A., Guha Biswas, P., and De Guzman, R.N. (2019). The type III secretion system needle, tip, and translocon. Protein Sci. Publ. Protein Soc. *28*, 1582–1593. 10.1002/pro.3682.
25. Betts-Hampikian, H.J., and Fields, K.A. (2010). The Chlamydial Type III Secretion Mechanism: Revealing Cracks in a Tough Nut. Front. Microbiol. *1*. 10.3389/FMICB.2010.00114.
26. Dehoux, P., Flores, R., Dauga, C., Zhong, G., and Subtil, A. Multi-genome identification and characterization of chlamydiae-specific type III secretion substrates: the Inc proteins. BMC Genomics *12*. 10.1186/1471-2164-12-109.
27. Peters, J., Wilson, D.P., Myers, G., Timms, P., and Bavoil, P.M. (2005). Type III secretion à la Chlamydia. Trends Microbiol. *15*, 241–251. 10.1016/j.tim.2007.04.005.
28. Ferrell, J.C., and Fields, K.A. A working model for the type III secretion mechanism in Chlamydia. Microbes Infect. Inst. Pasteur *18*, 84–92. 10.1016/j.micinf.2015.10.006.
29. Lutter, E.I., Martens, C., and Hackstadt, T. Evolution and conservation of predicted inclusion membrane proteins in chlamydiae. Comp. Funct. Genomics *2012*. 10.1155/2012/362104.
30. Rockey, D.D., Scidmore, M.A., Bannantine, J.P., and Brown, W.J. (2002). Proteins in the chlamydial inclusion membrane. Microbes Infect. *4*, 333–340. 10.1016/S1286-4579(02)01546-0.
31. Stanhope, R., Flora, E., Bayne, C., and Derré, I. (2017). IncV, a FFAT motif-containing Chlamydia protein, tethers the endoplasmic reticulum to the pathogen-containing vacuole. Proc. Natl. Acad. Sci. *114*, 12039–12044. 10.1073/PNAS.1709060114.
32. Luís, M.P., Pereira, I.S., Bugalhão, J.N., Simões, C.N., Mota, C., Romão, M.J., and Mota, L.J. (2023). The Chlamydia trachomatis IncM Protein Interferes with Host Cell Cytokinesis, Centrosome Positioning, and Golgi Distribution and Contributes to the Stability of the Pathogen-Containing Vacuole. Infect. Immun. *91*, e0040522. 10.1128/iai.00405-22.
33. Rosario, C.J., Hanson, B.R., and Tan, M. The transcriptional repressor EUO regulates both subsets of Chlamydia late genes. Mol. Microbiol. *94*, 888–897. 10.1111/mmi.12804.
34. Hatch, N.D., and Ouellette, S.P. (2023). Identification of the alternative sigma factor regulons of Chlamydia trachomatis using multiplexed CRISPR interference. bioRxiv. 10.1101/2023.04.27.538638.
35. Howard, L., Orenstein, N.S., and King, N.W. (1970). Purification on renografin density gradients of Chlamydia trachomatis grown in the yolk sac of eggs. Appl. Microbiol. *27*, 102–106.
36. Derré, I., Swiss, R., and Agaisse, H. (2011). The lipid transfer protein CERT interacts with the Chlamydia inclusion protein IncD and participates to ER-Chlamydia inclusion membrane contact sites. PLoS Pathog. *7*. 10.1371/JOURNAL.PPAT.1002092.
37. Anders, S., Pyl, P.T., and Huber, W. HTSeq–a Python framework to work with high-throughput sequencing data. Bioinforma. Oxf. Engl. *31*, 166–169. 10.1093/bioinformatics/btu638.
38. Shukla, X.U., and Parmar, D.J. (2014). Python – A comprehensive yet free programming language for statisticians. J. Stat. Manag. Syst. *19*, 277–284. 10.1080/09720510.2015.1103446.

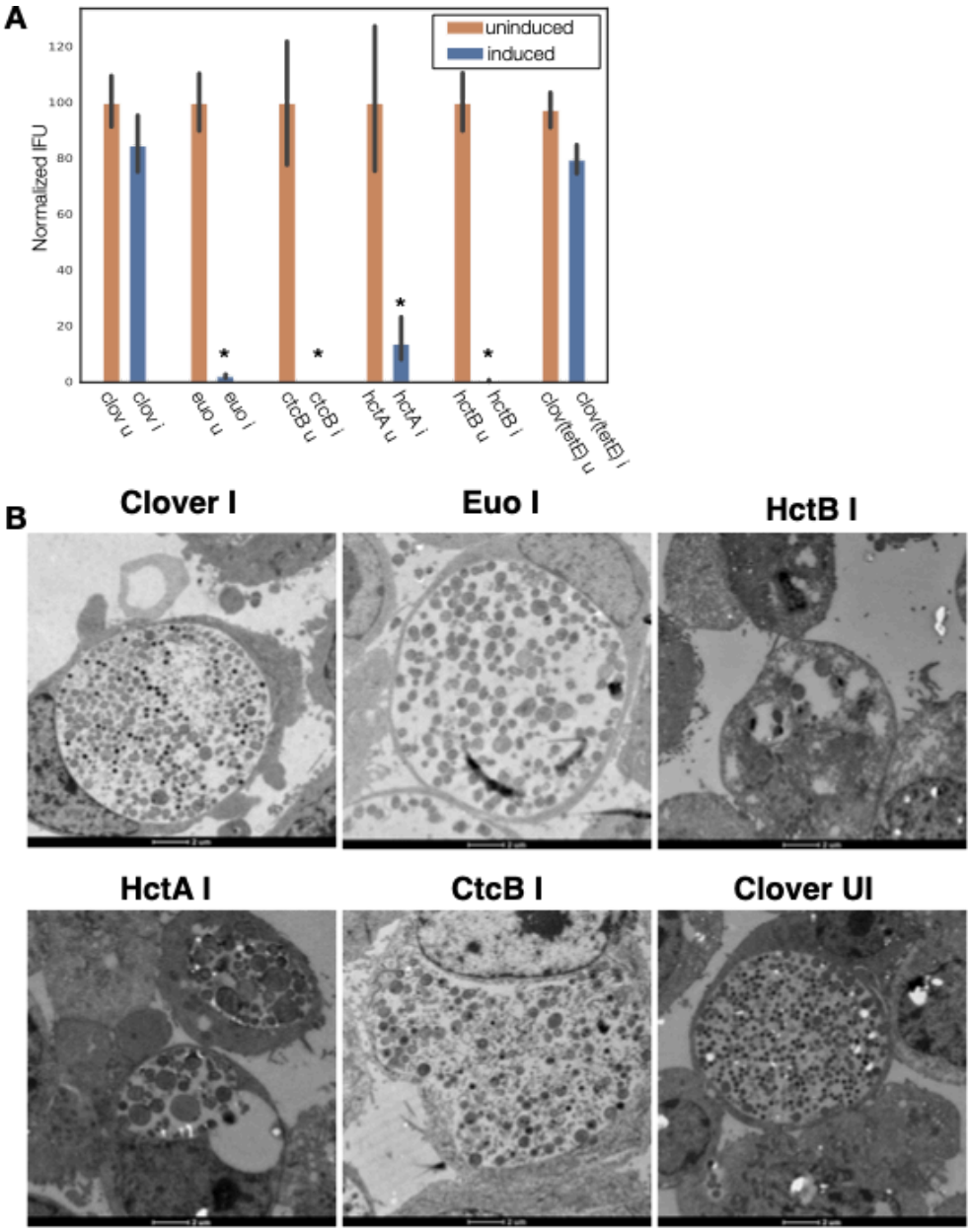

Figure 1. Ectopic expression of Euo, HctA, CtcB and HctB resulted in inhibition of the developmental cycle. **(**A) IFU production was dramatically reduced by the ectopic expression of Euo, HctA, CtcB and HctB but not by the expression of the Clover protein. * = $P < 0.01$. (B) Transmission EM of Cos-7 cells infected with *Ctr* expressing Clover, Euo, HctB, HctA or CtcB. The bacteria in the Clover induced and uninduced chlamydial infections looked similar with inclusions of both samples containing large RB like cells as well as electron dense EB like cells. The *Ctr* in the Euo expressing inclusions were primarily RB like cells while very few cells were electron dense EB cells. The chlamydial cells in the HctB expressing inclusions were aberrant looking, some with apparent condensed nucleoids. The HctA expressing *Ctr* also appeared aberrant with condensed nucleoids. Many of the CtcB expressing *Ctr* cells were target-like RB sized cells with a condensed nucleoid.

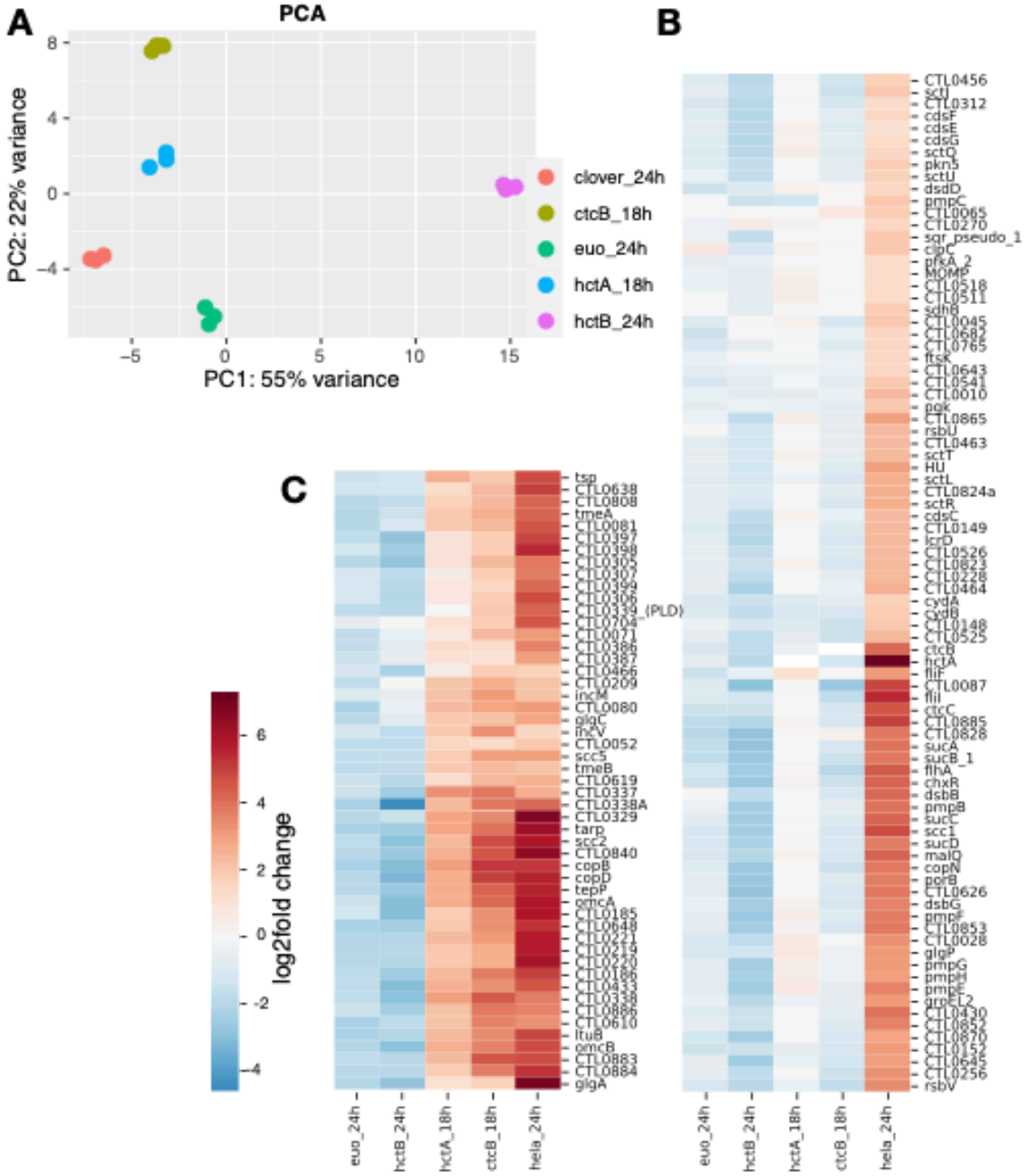

Figure 2. RNA-seq analysis of *Ctr* ectopically expressing Euo, HctA, HctB, or CtcB. **(**A) For each of the induced samples (n=3) the RNA-seq PCA profiles clustered within the same ectopic expression group but each group had a distinct profile as visualized by plotting the first and second principal component. Cluster plots of the log2fold expression changes as compared to the Clover control after the ectopic expression of the regulatory proteins, Euo, HctA, CtcB and HctA. The cluster plots revealed two distinct late gene regulation groups. (B) Cluster of genes that were upregulated between wt *Ctr* infections at 18 hpi and 24 hpi and upregulated by the ectopic expression of HctA and CtcB. (C) The second cluster consists of genes that are upregulated between wt *Ctr* infections at 18 hpi and 24 hpi but were not induced by ectopic expression of HctA and CtcB.

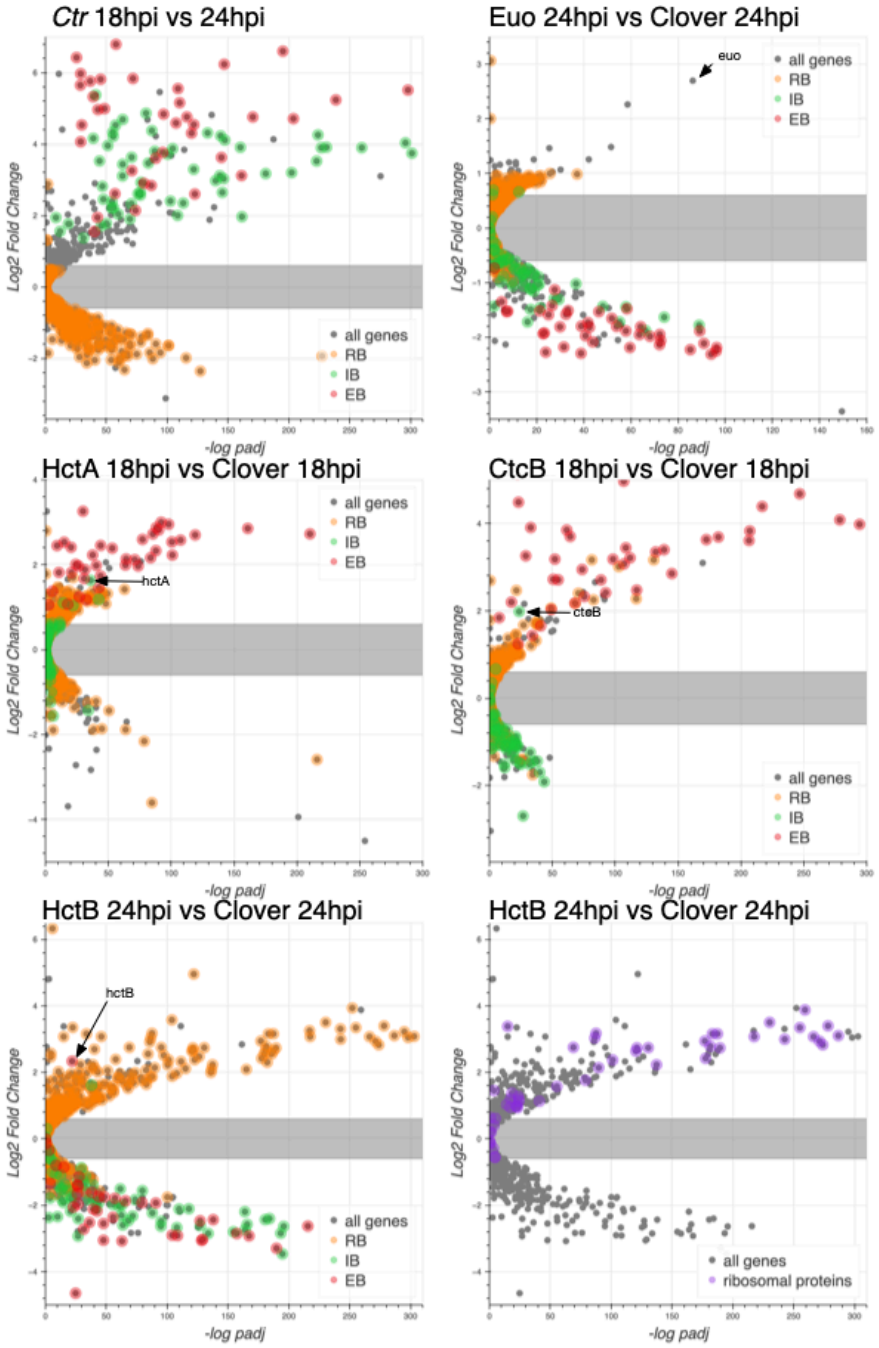

Figure 3. Effects of ectopic expression of Euo, HctA, CtcB and HctB on the gene expression of every Ctr gene. RNA-seq differential expression was determined for each gene using DESeq2 for native infection at 18hpi vs 24 hpi, Euo-FLAG expression, HctA-FLAG expression, CtcB-FLAG expression and HctB-FLAG expression vs the control Clover-FLAG. Volcano plots show that the expression of RB designated genes (orange) were largely unchanged from 18 hpi to 24 hpi while IB (green) and EB (red) designated genes were dramatically up regulated. For Euo-FLAG expression the RB genes (orange) were largely unchanged while IB genes (green) and EB genes (red) were all down regulated. Ectopic expression of HctA-FLAG resulted in the repression of many of the RB genes (orange) and up regulation of the EB genes (red) but had little impact on the expression of the IB genes (green). CtcB-FLAG expression had very little effect on RB genes (orange) but dramatically upregulated EB genes (red). The ectopic expression of HctB-FLAG resulted in the down regulation of both IB (green) and EB (red) genes but up-regulated many RB genes (orange). Additionally, HctB-FLAG expression resulted in the upregulation of many of the ribosomal protein genes (purple).

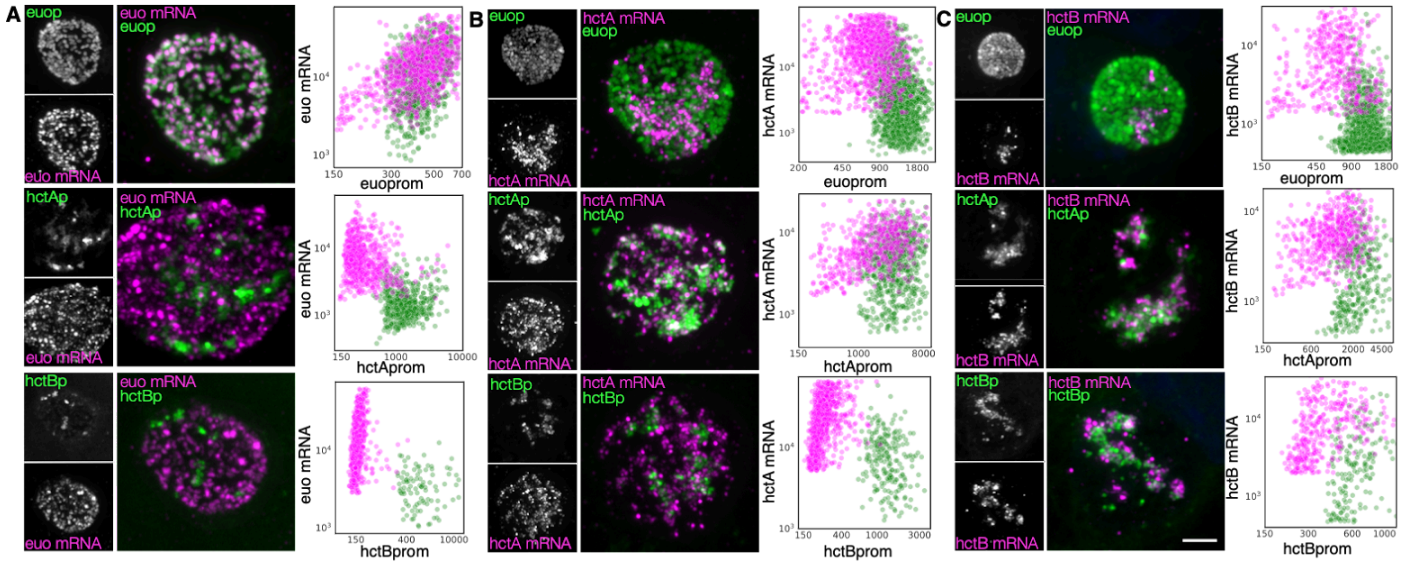

Figure 4. Cell type expression of representative genes from the three gene categories (RB, IB and EB) correspond to the three chlamydial cell forms. Cos-7 cells infected with L2-AsciEng or L2-BsciEng, fixed at 24 hpi and stained using FISH probes for *euo* mRNA, *hctA* mRNA and *hctB* mRNA. (A) Z-projection confocal micrographs showing *euo* mRNA localization in comparison to *euo*prom, *hctA*prom and *hctB*prom activity. Individual chlamydial cells with *euo* mRNA signal (pink) were identified using TrackMate and the fluorescence intensity for each channel (mRNA and promoter reporter) was plotted. Individual chlamydial cells positive for *euo*prom, *hctA*prom or *hctB*prom signal (green) were also identified using TrackMate and their expression intensity for each channel was plotted. (B) Z-projection confocal micrographs showing *hctA* mRNA localization in comparison to *euo*prom, *hctA*prom and *hctB*prom activity. Individual chlamydial cells with *hctA* mRNA signal (pink) were identified using TrackMate and the fluorescence intensity for each channel (mRNA and promoter reporter) was plotted. Individual chlamydial cells positive for *euo*prom, *hctA*prom or *hctB*prom signal (green) were also identified using TrackMate and their expression intensity for each channel was plotted. (C) Z-projection confocal micrographs showing *hctB* mRNA localization in comparison to *euo*prom, *hctA*prom and *hctB*prom activity. Individual chlamydial cells with *hctB* mRNA signal (pink) were identified using TrackMate and the fluorescence intensity for each channel (mRNA and promoter reporter) was plotted. Individual chlamydial cells positive for *euo*prom, *hctA*prom or *hctB*prom signal (green) were also identified using TrackMate and their expression intensity for each channel was plotted. Size bar = 5μm.

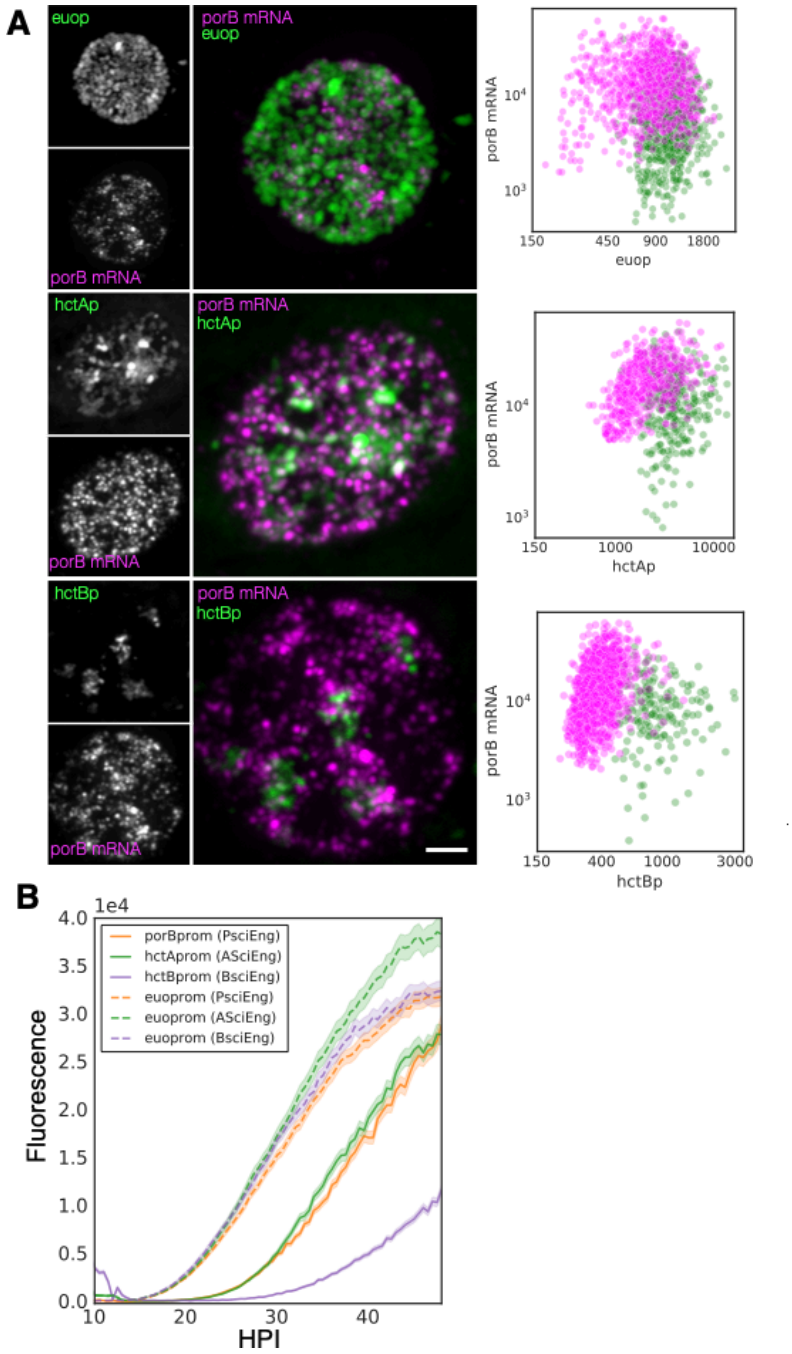

Figure 5. PorB gene expression is consistent with being classified as an IB gene. **(**A) FISH analysis of *porB* mRNA expression in comparison to *euo*prom, *hctA*prom and *hctB*prom activity at 24 hpi. Confocal micrographs of L2-AsciEng and L2-BsciEng infected cells probed for *porB* mRNA expression using Molecular instruments FISH probes. TrackMate was used to identify the *porB* mRNA+ cell population (pink) and measure the FISH fluorescent signal as well as the *euop*rom, *hctA*prom and *hctB*prom fluorescent signal. The intensity for both channels for each cell was plotted. The *euo*prom, *hctA*prom and *hctB*prom+ cell population were also identified (green) using TrackMate and the signal from the FISH channel and fluorescent protein channels were plotted on the same graphs. (B) Cells were infected with L2-PsciEng and the developmental gene expression kinetics were compared to those of L2-AsciEng, and L2-BsciEng. For all strains. The *euo*prom expression kinetics were comparable for all strains with expression first detected at ~15 hpi. *PorB*prom expression kinetics were nearly identical to *hctA*prom expression kinetics first detected at ~20 hpi while *hctB*prom expression was initiated at ~26 hpi. Error cloud for fluorescent reporters represents SEM. n > 20 inclusions per strain.

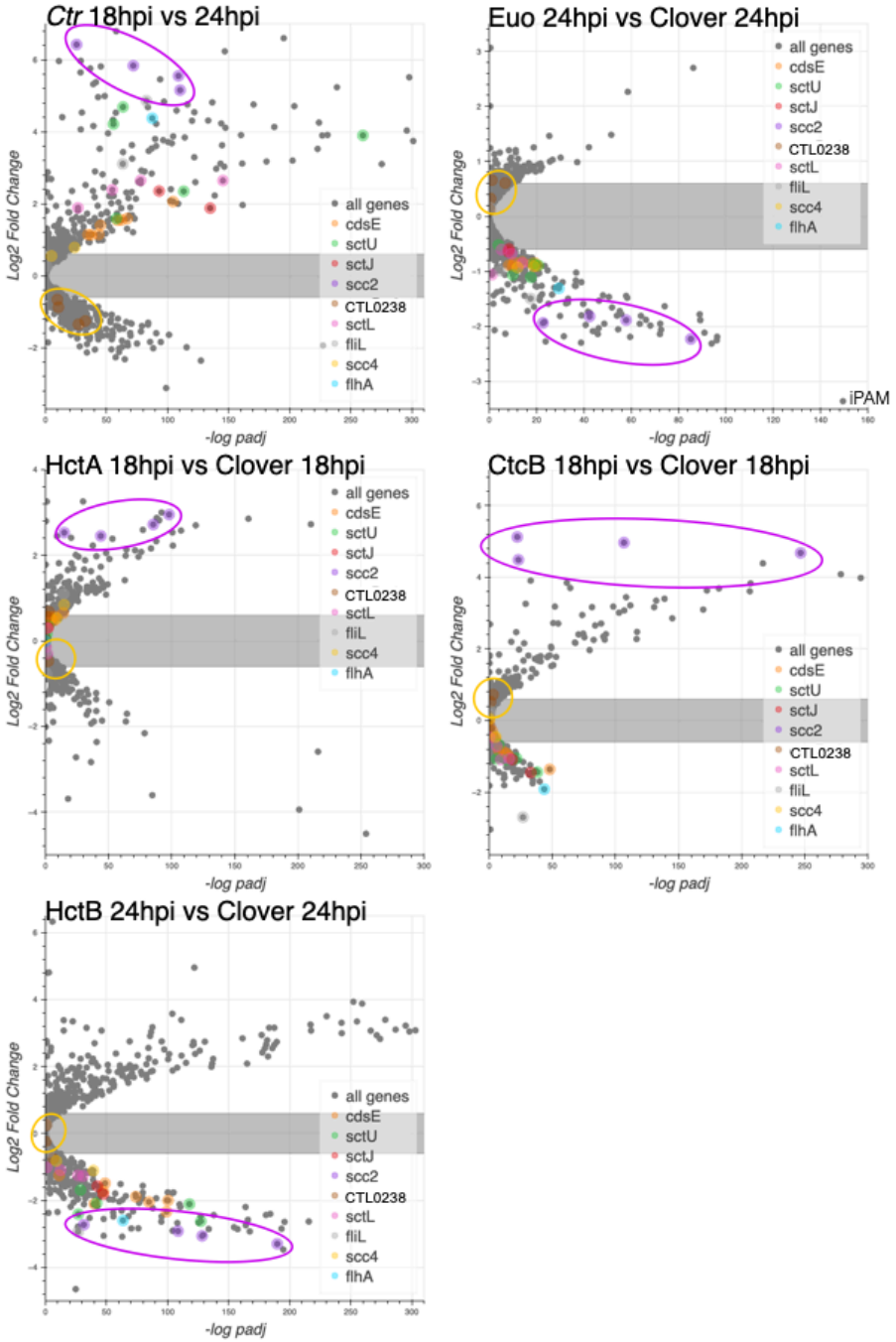

Figure 6. The effects of ectopic expression of Euo, HctA, CtcB and HctB on T3SS structural genes. The log2fold change RNA-seq differential expression data from the ectopic expression experiments were plotted against the -log of the p value (-log padj) and the operons for the T3SS were highlighted. For the wt *Ctr* 18 hpi vs 24 hpi samples most of the T3SS structural genes were upregulated while for the Euo ectopic expression experiment most of these operons were downregulated. Again, like the IB genes in the HctA and CtcB ectopic expression experiments, most of the structural genes were downregulated or unchanged. Two operons did not follow this pattern, the *CTL0238*-op and *scc2*-op. Both operons encode the components of the T3SS translocon. The *CTL0238*-op (gold circle) was regulaged like an RB gene while the *scc2*-op (purple circle) was regulated like an EB gene.

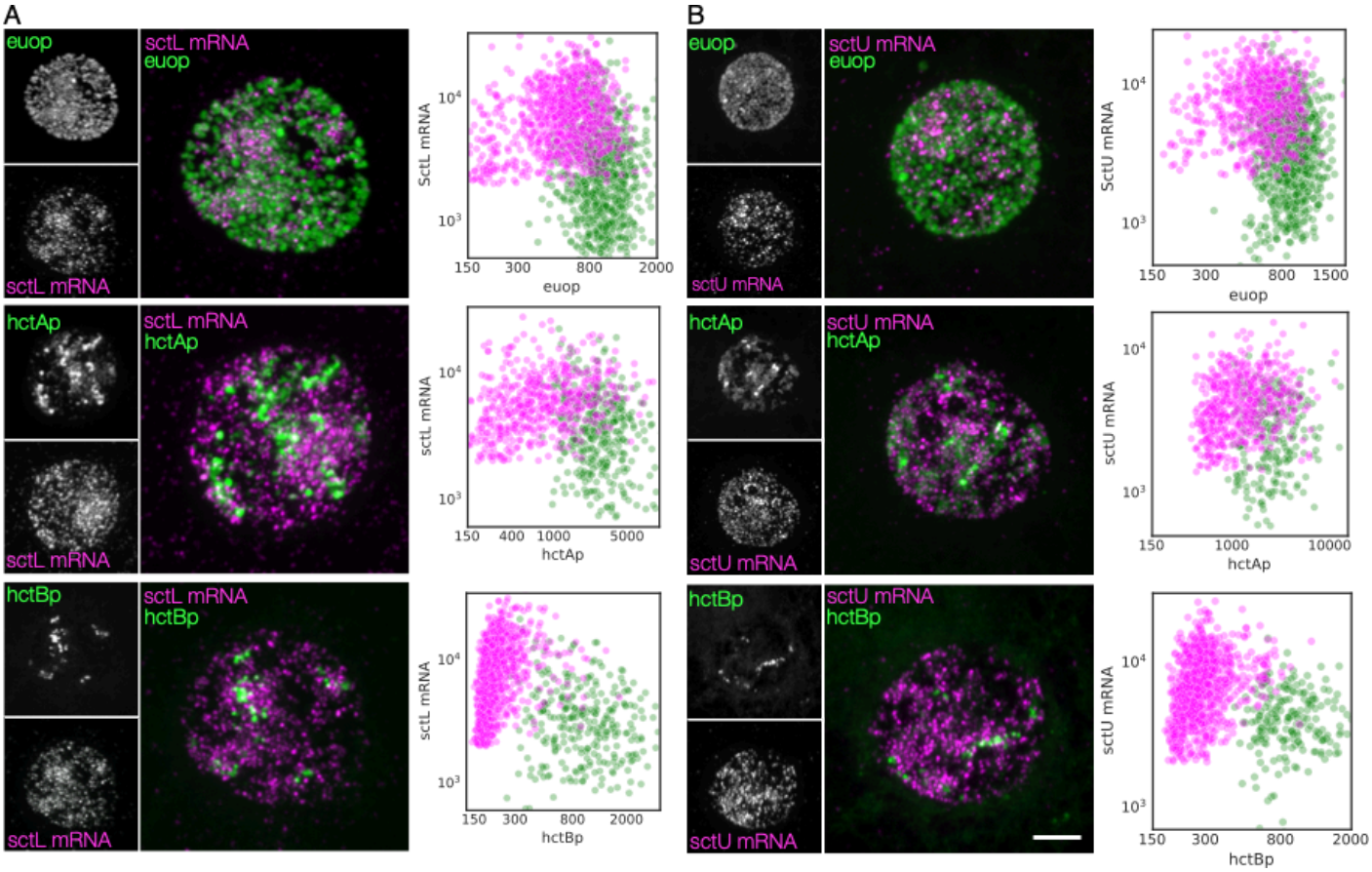

Figure 7. IB cell type expression of structural components of the T3SS. Confocal micrographs of Cos-7 cells infected with L2-AsciEng and L2-BsciEng for 24 hpi. Cells were stained using FISH probes to two T3SS structural operons, *sctL*-op and sctU-op. **(**A**) SctL-op.** For the *euo*prom signal the *sctL*-op FISH signal (pink) was present in a distinct subset of cells and not in the majority of the *euo*prom+ cells (green). TrackMate was used to identify the *sctL*-op mRNA+ cells and the signal for *euo*prom and FISH were quantified for each *sctL*-op+ cell. The converse was also performed, the *euo*prom+ cells were identified (green) and the *euo*prom signal and FISH signal was quantified for each *euo*prom+ cell. The fluorescence intensity for each channel for both cell populations was plotted. The FISH signal was also compared to the *hctA*prom expression pattern and showed subsets of cells that were stained for both *sctL*-op mRNA and *hctA*prom expression as well as non overlapping populations. The *sctL*-op mRNA+ cells were again identified using TrackMate (pink) and the signal for *hctA*prom and FISH were quantified for each *sctL*-op+ cell. Each *hctA*prom+ cell was also identified (green) and the FISH and *hctA*prom signal was determined and plotted for both cell populations. The *sctL* FISH staining was also compared to the expression form the *hctB*prom reporter. The *sctL*-op mRNA FISH staining was again present in a subset of cells but showed little overlap with the *hctB*prom fluorescent signal. The FISH signal and *hctB*prom signal were again measured in both cell populations (*sctL* mRNA+ cells (pink) and *hctB*prom+ cells (green)) and plotted. Both populations were primary single positive, either *sctL*-op mRNA high or *hctB*rpom high but rarely both. (B) ***SctU*-op.** The same analysis was performed for the *sctU*-op. The confocal images and individual cell expression plots showed a very similar pattern. Size bar = 5μm.

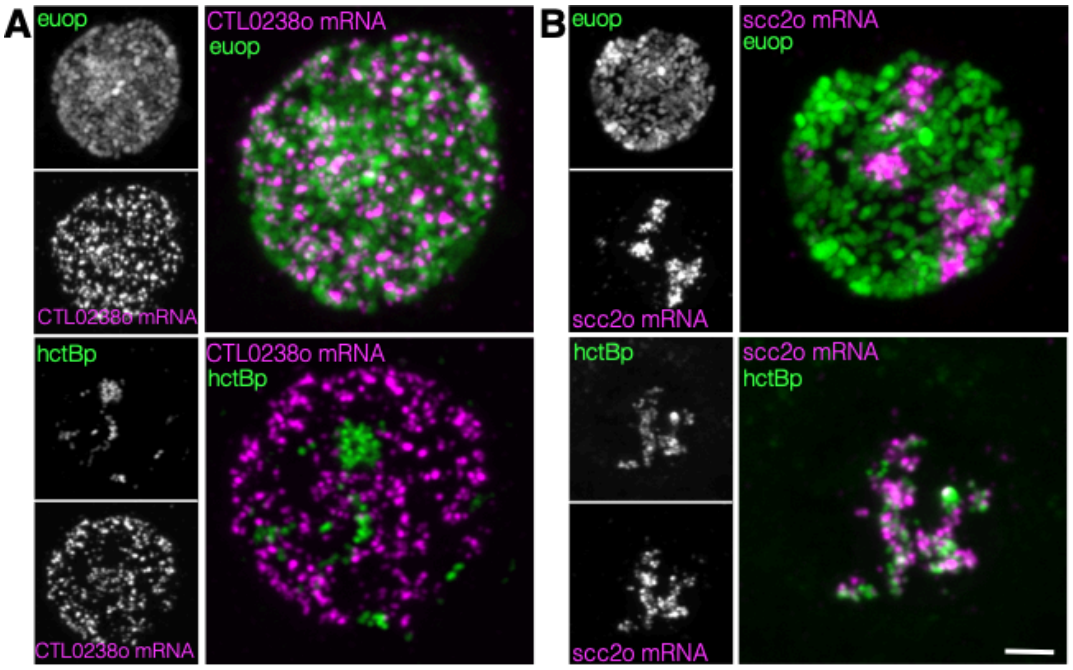

Figure 8. Cell type expression of the two T3SS translocons. A) Cos-7 cells were infected with L2-BsciEng for 24 hpi and stained for the mRNA expression of the *CTL0238*-op or the *scc2*-op using custom FISH probes. *Euo*prom expression (green) had significant overlap with *CTL0238*-op mRNA signal. For the *hctB*prom signal (green) there was little overlap with the *CTL0238*-op mRNA staining. B) For the *scc2*-op the FISH signal (pink) was in a cell population distinct from the majority of the *euo*prom signal (green). The *scc2*-op signal (pink) overlapped with *hctB*prom expression activity (green). Size bar = 5μm.

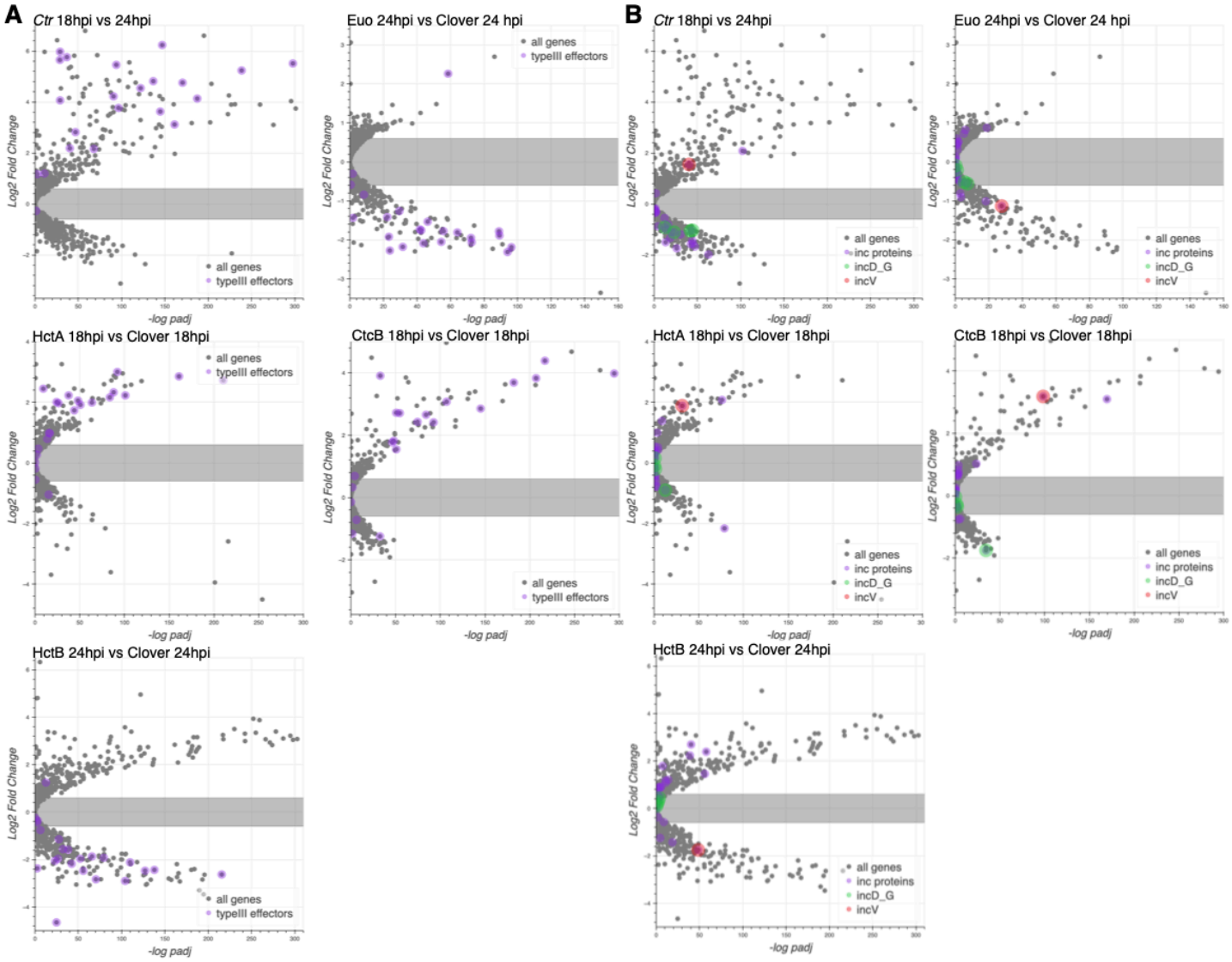

Figure 9. Effects of ectopic expression of Euo, HctA, CtcB and HctB on the expression of T3SS effectors. RNA-seq differential expression data (log2fold change) plotted vs the - log of the P value (-log padJ) for *Ctr* ectopically expressing Euo, HctA, CtcB and HctB. **(A)** The T3SS effectors are highlighted in purple. (B) All the *inc* protein genes are highlighted in purple while the genes for the *incD-G* operon are highlighted in green and *incV* is highlighted in red.

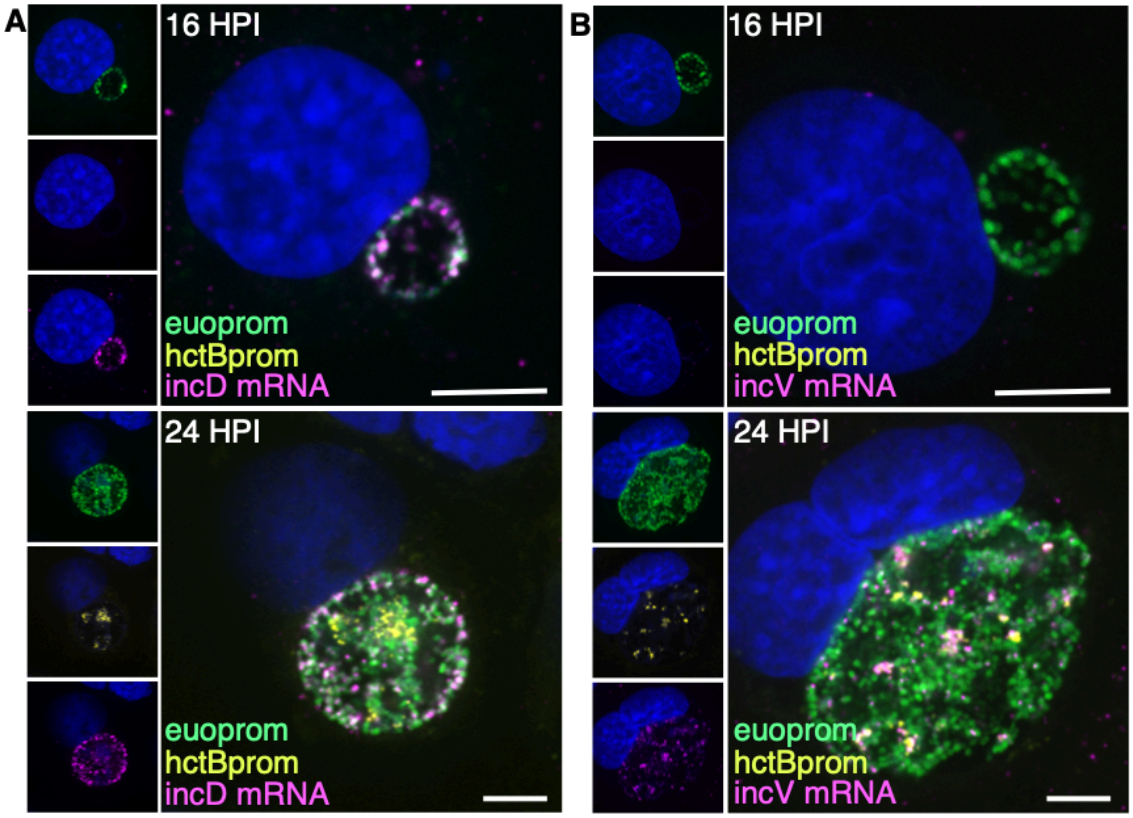

Figure 10. Cell type expression of *incD* and *incV*. Cos-7 cells infected with L2-BsciEng for 16 and 24 hpi and stained for *incD* and *incV* mRNA expression using custom FISH probes. (A) The *incD* mRNA (pink) was visibly expressed in the *euo*prom+ (green) RB cells at 16 hpi while *hctB*prom signal was not detected. At 24 hpi the *incD* mRNA signal (pink) overlapped with the *euo*prom signal (green) but was separate from the *hctB*prom+ cells (yellow). (B) The *incV* mRNA signal (pink) was undetected at 16 hpi. At 24 hpi the *incV* mRNA signal showed overlap with the *hctB*prom signal (yellow) but not the *euo*prom signal (green). Size bar = 5μm.

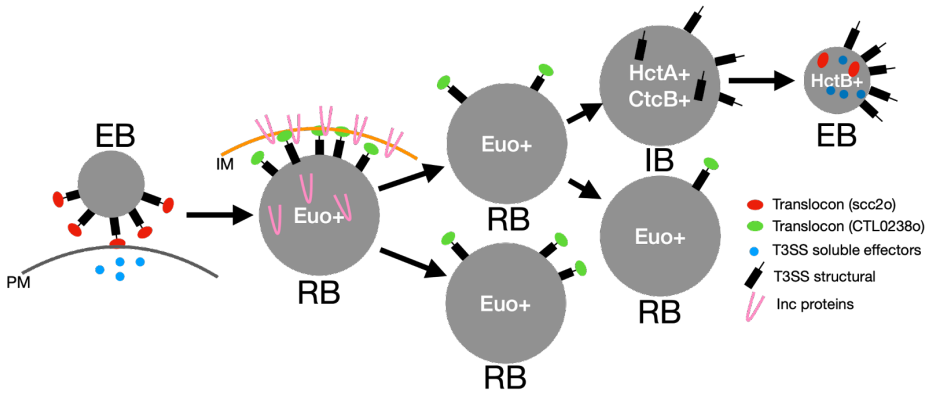

Figure 11. Model of cell type specific deployment of the T3SS. In this model the *scc2*-op translocon secretes effectors across the plasma membrane (PM) for host cell entry. The *scc2*-op translocon is replaced in the RB with the *CTL0239*-op translocon for the secretion of the Inc proteins across the inclusion membrane (IM). The structural components of the T3SS are then reconstructed during the IB to EB maturation phase.

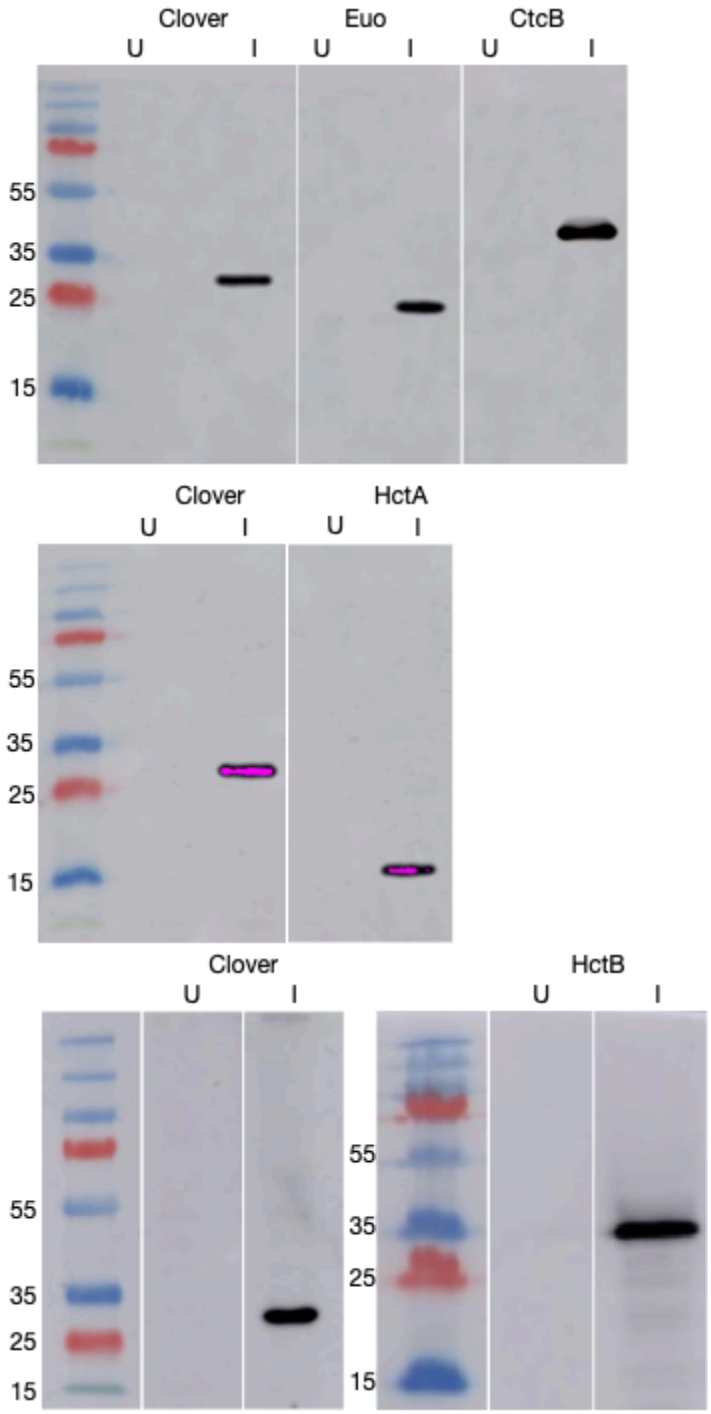

Fig S1. Western analysis of ectopically expressed Clover, Euo, HctA, CtcB and HctB.
To ensure the FLAG constructs expressed protein of the correct size, infected and induced monolayers were lysed in reducing lane marker sample buffer and protein lysates were separated on 10% SDS-PAGE gels and transferred to a nitrocellulose membrane for western analysis of the FLAG-tagged protein. The membrane was blocked with PBS + 0.1% Tween 20 (PBS-T) and 5% nonfat milk prior to incubating in either monoclonal anti-FLAG M2 antibody (1:40,000, Sigma, Thermo Scientific™) overnight at 4 ºC followed by goat-anti mouse IgG-HRP secondary antibody (Invitrogen™) at room temperature for 2 hours. The membrane was developed with the Supersignal West Dura luminol and peroxide solution (Thermo Scientific™) and imaged using an Amersham Imager 600.

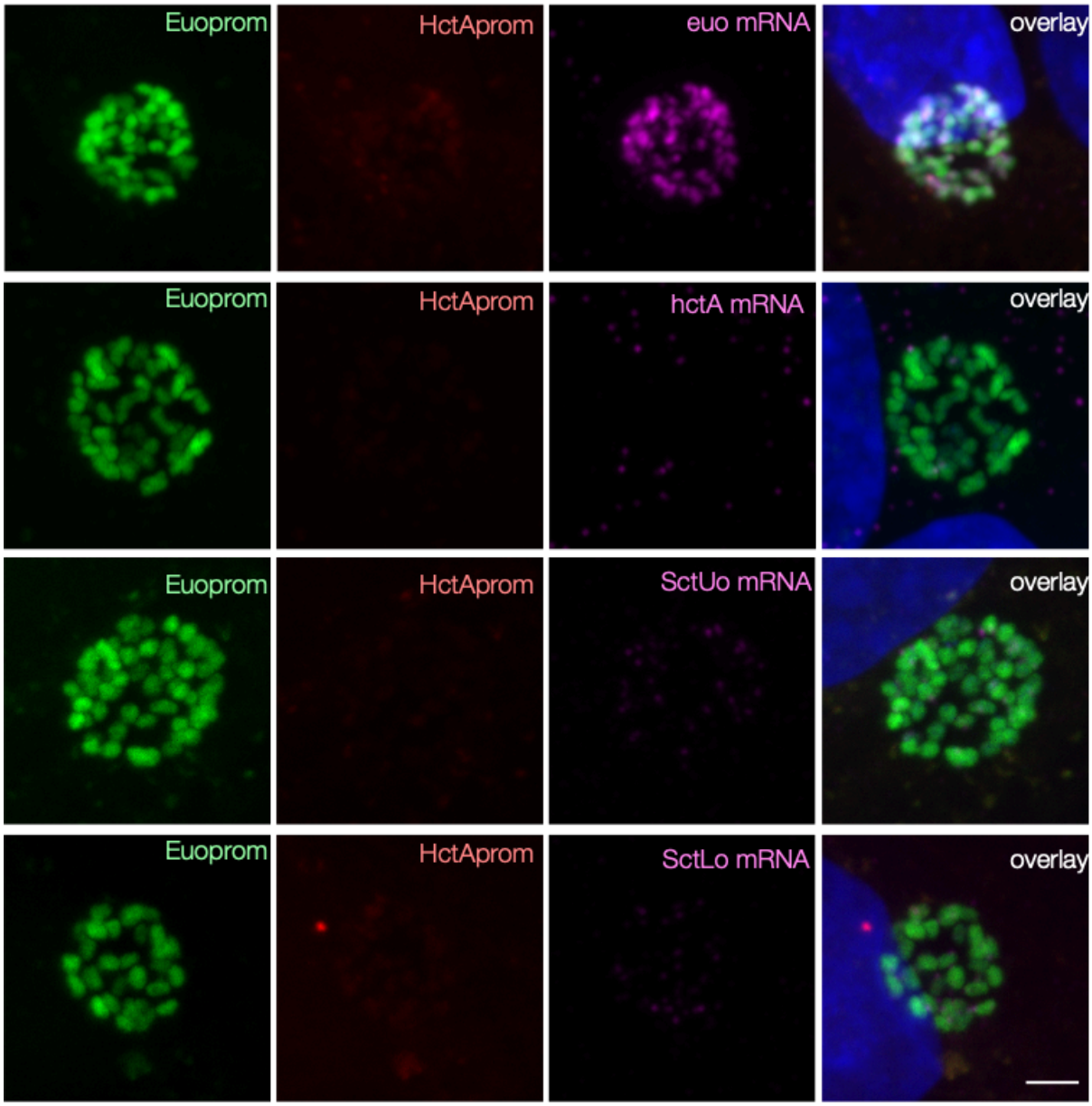

Fig S2. Confocal Z projection micrographs of Cos-7 cells infected with L2-AsciEng and fixed at 16 hpi. Cells were stained with FISH probes to visualize mRNAs for *euo*, *hctA, sctU*-op and *sctL*-op (pink). The *euo*prom drove the expression of Neongreen fluorescent protein (green) while the *hctA*prom drove the expression of the scarlet-I fluorescent protein (red). Size bar = 5μm.

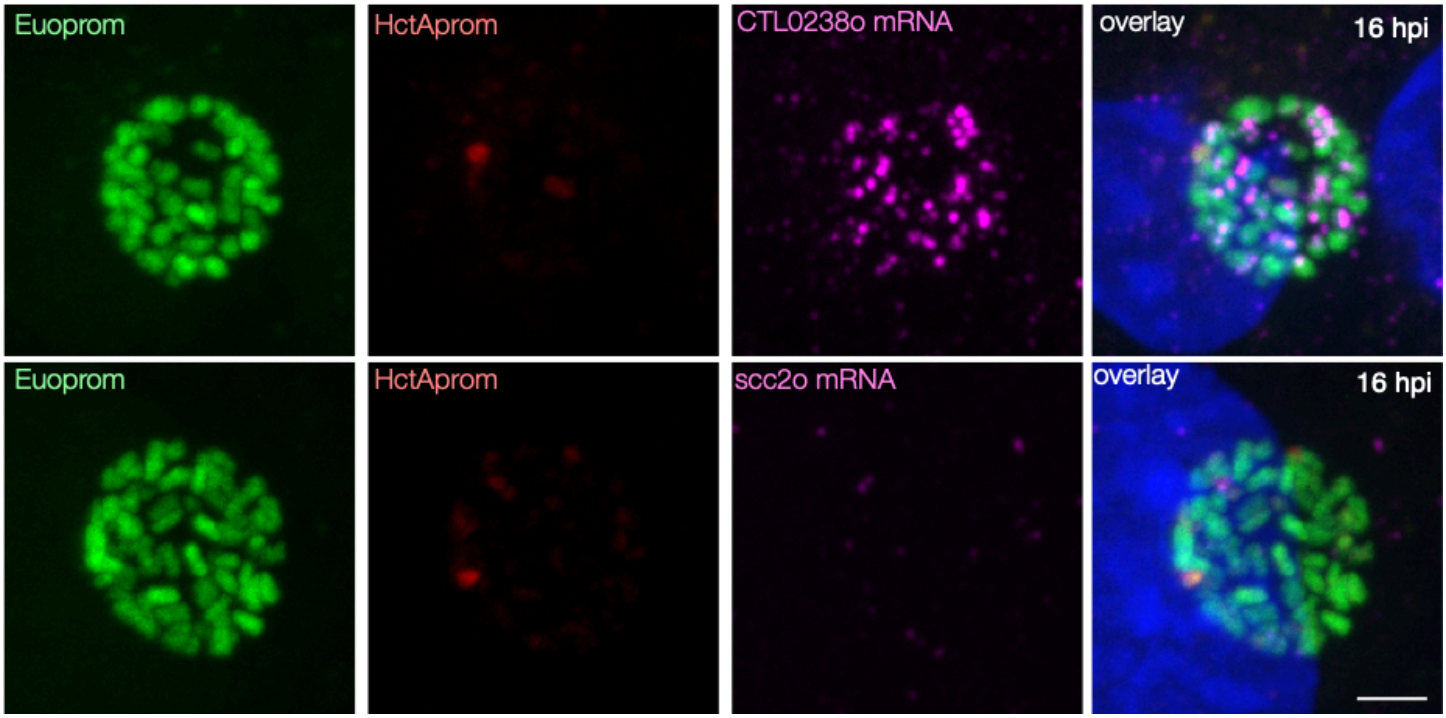

Fig S3. Confocal Z projection micrographs of Cos-7 cells infected with L2-AsciEng and fixed at 16 hpi. Cells were stained with FISH probes to visualize mRNAs for the *CTL0238*-op and the *scc2*-op (pink). The *euo*prom drove the expression of Neongreen fluorescent protein (green) while the *hctA*prom drove the expression of the scarlet-I fluorescent protein (red). Size bar = 5μm.

Supplemental tables

Table S1. Chlamydial genes designated as RB, IB, EB expressed genes and their regulation from ectopic expression of Euo, HctA, CtcB and HctB

Table S2. T3SS structural operons.

Table S3. T3SS effector gene regulation from ectopic expression of Euo, HctA, CtcB and HctB.

Table S4. Inc gene regulation from ectopic expression of Euo, HctA, CtcB and HctB.

Table S5. List of primers used to construct plasmids

Table S6. List of FISH probes and the location on the *Ctr* genome

Table S1 Cell type categorization

gene_name	gene_num	18hpi vs 24hpi	euo 24h vs clover 24h	hctA 18h vs clover 18h	ctcB_18h vs clover 18h	hctB_24h vs clover 24h	cell_type
hemB	CTL0001	-0.30	0.00	0.41	0.00	0.50	RB
greA	CTL0004	-0.87	0.31	0.81	0.86	1.04	RB
aspC_1	CTL0005	-0.74	0.35	0.79	0.56	0.89	RB
mreC	CTL0006	-0.31	0.40	0.00	0.00	0.52	RB
CTL0009	CTL0009	-1.53	0.00	0.99	1.19	0.86	RB
CTL0012	CTL0012	-1.16	0.00	0.64	1.46	1.41	RB
CTL0013	CTL0013	-1.49	0.00	1.30	0.00	3.07	RB
CTL0014	CTL0014	-1.47	0.00	1.39	3.17	2.11	RB
CTL0015	CTL0015	-2.13	0.00	1.43	3.17	1.76	RB
CTL0016	CTL0016	-1.60	0.35	1.21	3.01	1.36	RB
CTL0017	CTL0017	-0.77	0.00	0.00	2.47	0.96	RB
CTL0019	CTL0019	-0.65	-0.74	0.00	0.00	0.00	RB
recD_1	CTL0020	0.47	0.00	-0.43	0.00	-1.02	RB
CTL0022	CTL0022	0.35	-0.43	0.00	-0.32	-0.99	RB
CTL0023	CTL0023	0.32	0.00	-0.58	0.00	-1.13	RB
parC	CTL0029	0.00	-0.53	0.59	0.47	-0.58	RB
parE	CTL0030	0.00	0.57	0.00	-0.63	0.00	RB
hemA	CTL0031	-0.43	-0.39	0.00	0.31	0.00	RB
frr	CTL0046	-1.26	0.79	0.83	1.03	0.35	RB
pyrH	CTL0047	-1.21	0.51	0.86	0.97	0.00	RB
tsf	CTL0048	-1.21	0.51	0.78	0.60	0.00	RB
rpsB	CTL0049	-1.02	0.44	0.59	0.42	0.00	RB
sulB	CTL0053	-0.94	0.00	-0.39	-0.95	-0.25	RB
sufC	CTL0054	-0.45	0.00	0.00	-0.78	0.00	RB
sufD	CTL0055	-0.49	0.00	0.00	-0.68	0.00	RB
sufS	CTL0056	-0.35	0.34	0.00	-0.27	0.26	RB
parB	CTL0057	0.00	0.31	-0.65	0.00	0.54	RB
dppF	CTL0058	0.21	0.83	-1.10	-0.33	0.91	RB
dppD	CTL0059	-0.95	0.00	-1.88	-0.76	1.83	RB
CTL0060	CTL0060	-1.33	0.35	0.00	0.50	2.30	RB
CTL0061	CTL0061	-0.99	0.00	-0.52	0.00	1.65	RB
trmE	CTL0067	-0.50	0.00	0.00	0.00	0.00	RB
psdD	CTL0068	-0.33	0.00	0.00	-0.50	-0.72	RB
secA	CTL0070	0.00	0.00	0.00	0.26	-0.91	RB
engA	CTL0072	-0.72	0.55	0.00	0.00	2.05	RB
pcnB_1	CTL0073	0.18	0.48	-0.36	0.00	1.43	RB
clpX	CTL0074	-0.29	0.28	-0.67	0.00	1.24	RB
clpP_1	CTL0075	-0.34	0.00	-1.36	-0.99	0.85	RB
tig	CTL0076	-1.39	0.25	-0.33	0.34	1.75	RB
CTL0090	CTL0090	0.00	0.00	-0.66	0.00	0.00	RB
rluB	CTL0092	-1.25	0.00	0.42	0.31	1.44	RB
CTL0093	CTL0093	0.00	-0.60	-0.57	-0.78	-0.97	RB
CTL0097	CTL0097	0.42	0.00	-0.74	-0.40	-0.55	RB
serS	CTL0098	0.00	0.00	-0.95	-0.25	0.00	RB
ribD	CTL0099	-0.60	0.61	-0.63	0.00	0.00	RB
ribA	CTL0100	-0.67	0.00	-0.51	0.00	0.28	RB
ribH	CTL0101	0.00	0.00	-0.99	-0.71	0.00	RB

CTL0103	CTL0103	0.34	-0.34	0.00	0.27	0.50	RB
dagA	CTL0104	0.40	0.00	0.00	0.00	0.77	RB
yajC	CTL0110	0.00	0.31	-0.92	-0.75	-0.87	RB
CTL0111	CTL0111	-0.68	0.00	0.35	0.00	1.42	RB
hemN_1	CTL0115	0.35	0.53	0.00	0.00	1.93	RB
hemE	CTL0116	0.24	0.58	0.00	0.00	2.51	RB
mfd	CTL0117	-0.54	0.59	0.44	0.45	2.54	RB
alaS	CTL0118	-0.59	0.51	0.00	-0.26	1.99	RB
tktB	CTL0119	-0.85	0.97	1.14	0.74	2.38	RB
efp_1	CTL0121	-0.86	0.88	0.32	0.00	2.22	RB
groEL_1	CTL0124	0.44	0.00	0.00	-0.46	0.82	RB
mraY	CTL0126	0.00	0.00	0.00	0.00	1.05	RB
murD	CTL0127	0.45	0.33	0.00	0.00	0.46	RB
nlpD	CTL0128	0.45	0.00	-0.50	-0.33	-0.44	RB
murC	CTL0131	-0.36	0.51	-0.71	0.00	0.00	RB
CTL0132	CTL0132	0.00	0.96	-3.60	0.00	0.00	RB
CTL0137	CTL0137	-1.11	0.76	0.00	0.50	0.31	RB
CTL0138	CTL0138	-0.31	0.72	-0.39	0.00	0.00	RB
fabF	CTL0139	-0.52	0.28	-0.78	0.00	-0.74	RB
CTL0140	CTL0140	-0.47	0.64	-0.46	0.00	-0.40	RB
ppa	CTL0141	-0.84	0.89	-0.43	0.67	0.86	RB
ldh	CTL0142	-0.74	0.00	-1.88	0.56	0.00	RB
cysQ	CTL0143	0.00	0.00	-0.63	0.00	0.00	RB
CTL0144	CTL0144	0.18	0.00	-0.32	0.49	-1.01	RB
aas	CTL0145	0.30	0.00	-0.22	0.47	-1.15	RB
bioF	CTL0146	-0.26	0.00	0.00	0.77	0.00	RB
lysS	CTL0150	-0.51	0.24	0.00	-0.31	-1.12	RB
cysS	CTL0151	0.00	0.00	-0.44	-0.39	0.85	RB
rnpA	CTL0153	-1.02	0.00	1.29	0.00	2.00	RB
rpmH	CTL0153A	-0.91	0.00	0.00	0.00	1.45	RB
rpmJ	CTL0154	-1.29	0.00	0.33	0.00	1.27	RB
rpsN	CTL0155	-1.24	0.00	0.00	0.00	1.12	RB
CTL0157	CTL0157	0.00	0.00	0.00	0.00	2.02	RB
CTL0163	CTL0163	-0.82	0.00	0.00	0.00	0.00	RB
glyQ	CTL0165	-0.90	0.68	0.00	0.00	-0.50	RB
rplY	CTL0168	-1.60	0.42	0.82	0.73	3.40	RB
pth	CTL0169	-1.67	0.00	0.71	0.97	2.91	RB
rpsF	CTL0170	-1.27	0.62	0.81	0.27	3.16	RB
rpsR	CTL0171	-1.35	0.50	0.77	0.00	2.75	RB
rplI	CTL0172	-1.43	0.51	0.83	0.69	2.63	RB
ispE	CTL0173	-1.34	0.00	0.00	0.00	3.57	RB
plsB	CTL0176	0.00	0.00	-0.33	0.00	0.74	RB
cafE	CTL0177	-0.17	-0.51	-0.43	0.00	0.00	RB
CTL0178	CTL0178	-1.46	0.68	0.00	0.00	1.86	RB
CTL0179	CTL0179	-1.32	0.70	0.00	0.00	0.64	RB
rpmF	CTL0181	-0.69	0.00	0.00	0.56	0.00	RB
plsX	CTL0182	-1.05	0.65	0.00	0.60	0.53	RB
pmpD	CTL0183	-0.70	0.99	-2.59	0.48	0.24	RB
lnaC	CTL0184	-0.30	-0.33	-0.60	0.72	-0.37	RB

tyrP	CTL0189	-0.57	0.55	-0.80	0.49	0.63	RB
CTL0190	CTL0190	-0.46	0.54	-0.62	0.30	0.28	RB
ftsY	CTL0192	-0.47	-0.29	0.00	0.00	-0.88	RB
CTL0196	CTL0196	-0.22	0.38	-0.45	0.00	-1.14	RB
rmuC	CTL0197	0.00	0.00	-0.29	-0.29	-0.57	RB
pssA	CTL0198	0.33	-0.28	-0.51	-0.97	-1.44	RB
CTL0202	CTL0202	-0.73	0.00	0.00	0.00	3.07	RB
nusB	CTL0204	-0.65	0.00	-0.34	-0.67	2.64	RB
infC	CTL0205	-1.32	0.53	1.09	0.60	1.85	RB
rpmI	CTL0206	-0.89	0.00	0.00	0.00	0.00	RB
rplT	CTL0207	-1.22	0.00	1.04	0.63	1.20	RB
pheS	CTL0208	-1.05	0.31	0.78	0.59	1.51	RB
CTL0210	CTL0210	0.00	-0.73	0.77	0.99	0.95	RB
CTL0211	CTL0211	0.00	0.00	-0.58	0.00	0.37	RB
tilS	CTL0212	-0.36	0.00	-0.65	0.00	0.00	RB
pnp	CTL0214	-0.85	0.71	0.00	0.26	-0.40	RB
rpsO	CTL0215	-0.72	0.77	0.00	0.00	-0.57	RB
CTL0216	CTL0216	0.00	0.65	-1.58	0.00	0.86	RB
CTL0222	CTL0222	-1.48	0.84	0.60	0.47	0.00	RB
CTL0223	CTL0223	-0.17	0.00	0.00	-0.37	-1.43	RB
map	CTL0224	-0.57	0.48	0.00	0.00	-0.83	RB
CTL0225	CTL0225	-1.11	0.49	0.51	0.61	0.00	RB
CTL0226	CTL0226	-1.10	0.35	0.00	0.00	-0.34	RB
CTL0227	CTL0227	-0.85	0.75	-0.36	0.00	-0.41	RB
CTL0231	CTL0231	-0.31	0.00	0.32	0.00	-0.35	RB
CTL0231B	CTL0231b	0.00	0.00	0.00	-0.97	-1.68	RB
CTL0232	CTL0232	0.00	0.25	0.00	-0.40	-0.83	RB
ispH	CTL0234	-0.60	-0.32	-1.44	0.35	-0.83	RB
copD_2	CTL0235	-0.66	0.00	-0.47	0.00	0.00	RB
copB_2	CTL0236	-1.35	0.00	0.69	0.72	0.00	RB
scc3	CTL0237	-0.88	0.00	0.00	0.00	0.00	RB
CTL0238	CTL0238	-1.26	0.61	0.00	0.00	-0.76	RB
CTL0244	CTL0244	-0.70	0.00	-0.60	0.00	-0.68	RB
dub2	CTL0246	-0.32	0.00	0.55	2.06	0.00	RB
dub1	CTL0247	0.33	-0.26	0.27	0.71	-0.31	RB
pmpI	CTL0254	0.33	-0.30	-0.24	0.00	1.16	RB
gatC	CTL0257	-1.03	0.00	0.00	0.00	0.00	RB
gatA	CTL0258	-0.78	0.39	0.00	0.38	-0.42	RB
gatB	CTL0259	-0.53	0.44	0.00	0.44	-0.25	RB
CTL0261	CTL0261	-1.50	0.00	0.00	0.00	0.54	RB
CTL0262	CTL0262	-0.83	-0.97	-0.32	0.00	0.00	RB
rnhC	CTL0263	0.00	0.00	-0.50	-0.40	0.00	RB
CTL0264	CTL0264	0.38	0.36	-0.76	-0.84	-0.45	RB
htrB	CTL0265	-0.26	0.00	-0.90	-0.52	0.00	RB
CTL0266	CTL0266	-0.21	0.00	-0.80	0.00	-0.28	RB
dacA	CTL0267	-0.43	0.00	-0.85	0.00	-0.42	RB
CTL0273	CTL0273	-0.27	-0.60	1.05	1.70	0.00	RB
ileS	CTL0274	-0.85	0.96	0.86	0.81	0.82	RB
lepB	CTL0275	0.32	0.29	-0.69	-0.43	0.38	RB

rpmE2	CTL0277	-0.76	0.38	-0.61	-0.89	0.40	RB
prfA	CTL0278	-0.44	0.00	-0.46	-0.40	0.00	RB
CTL0279	CTL0279	-0.30	0.00	0.00	0.00	0.00	RB
ffh	CTL0280	-1.26	0.51	0.83	0.63	1.06	RB
rpsP	CTL0281	-1.84	0.66	0.82	0.34	1.03	RB
trmD	CTL0282	-1.84	0.64	1.25	0.95	1.07	RB
rplS	CTL0283	-1.65	0.69	0.94	0.54	0.61	RB
rnhB	CTL0284	-1.59	0.61	1.24	0.77	1.14	RB
gmk	CTL0285	-0.61	0.00	0.83	0.53	0.00	RB
CTL0286	CTL0286	-0.66	0.00	0.00	0.00	0.00	RB
metG	CTL0287	-0.78	0.00	0.51	0.41	0.00	RB
recD_2	CTL0288	-0.20	0.00	-0.28	0.00	0.00	RB
CTL0289	CTL0289	0.00	-0.37	-0.68	0.00	0.00	RB
CTL0290	CTL0290	0.00	-0.34	0.00	0.00	0.00	RB
CTL0291	CTL0291	-0.88	0.00	0.00	0.00	1.53	RB
CTL0292	CTL0292	0.00	0.00	0.00	0.00	1.73	RB
CTL0293	CTL0293	0.00	0.00	0.00	0.00	-1.65	RB
dcd	CTL0294	0.00	0.00	-1.23	-1.40	-1.45	RB
CTL0303	CTL0303	0.00	0.00	0.00	-0.65	0.00	RB
CTL0304	CTL0304	-1.01	0.00	0.00	-0.51	-0.59	RB
hemN_2	CTL0308	0.34	-0.58	0.34	0.63	-0.71	RB
CTL0309	CTL0309	0.33	-0.76	0.00	-0.41	-1.42	RB
ispG	CTL0313	-0.66	0.00	0.00	0.00	0.42	RB
CTL0314	CTL0314	-1.18	0.00	1.69	0.50	0.00	RB
fer	CTL0315	-1.07	0.31	0.86	0.45	-0.65	RB
tyrS	CTL0318	-0.52	0.52	-0.46	0.00	-1.05	RB
gnd	CTL0319	-0.23	0.49	-0.71	-0.24	-0.40	RB
lepA	CTL0320	-0.86	0.48	0.23	0.38	3.22	RB
CTL0321	CTL0321	0.00	0.00	-0.51	0.00	0.87	RB
ddbA	CTL0322	0.21	0.00	0.33	0.00	0.77	RB
ytgA	CTL0323	-0.25	0.00	-0.35	-0.46	0.62	RB
ytgB	CTL0324	0.00	0.00	0.27	0.00	1.07	RB
ytgC	CTL0325	-0.44	0.00	0.40	0.52	1.25	RB
ytgD	CTL0326	-0.28	0.00	0.00	0.49	1.25	RB
ispC	CTL0327	-0.18	0.36	0.47	0.50	1.70	RB
CTL0328	CTL0328	-0.34	0.45	0.00	0.25	1.63	RB
recF	CTL0330	0.00	0.00	0.64	0.92	1.34	RB
dnaN	CTL0331	0.00	0.00	0.00	-0.86	-0.93	RB
smpB	CTL0332	-0.30	0.00	0.00	0.00	0.83	RB
folD	CTL0334	0.00	0.00	-0.35	0.00	0.00	RB
CTL0340	CTL0340	-0.95	0.00	0.45	0.56	0.00	RB
rpmB	CTL0341	-1.20	0.57	0.00	0.00	-0.55	RB
engD	CTL0347	-0.67	0.00	-0.37	-0.38	0.00	RB
ribF	CTL0348	-1.03	0.65	0.00	0.00	0.91	RB
truB	CTL0349	-0.96	0.59	0.98	0.94	0.68	RB
rbfA	CTL0350	-1.24	0.80	0.73	0.86	0.00	RB
infB	CTL0351	-1.34	0.77	1.12	1.19	1.07	RB
nusA	CTL0352	-1.30	0.87	1.03	0.92	0.48	RB
rpsA	CTL0353	-1.34	0.84	0.65	0.58	-0.29	RB

trxB	CTL0354	-0.29	0.74	-0.39	-0.55	0.51	RB
acpS	CTL0355	-0.38	0.82	0.00	0.00	1.00	RB
CTL0356	CTL0356	-0.88	0.49	0.00	0.00	0.91	RB
CTL0361	CTL0361	-0.54	0.00	0.00	-0.74	1.16	RB
mutY	CTL0362	-1.01	0.79	0.00	0.00	1.17	RB
groEL_3	CTL0365	0.00	0.00	-0.95	0.00	0.00	RB
groES	CTL0366	0.00	0.00	-1.16	-0.77	0.00	RB
pepF	CTL0367	-0.32	0.40	-0.98	-0.90	1.28	RB
clpB	CTL0368	0.47	0.27	-0.75	-0.22	0.67	RB
incD	CTL0370	-1.05	-0.56	0.00	0.00	0.30	RB
incE	CTL0371	-0.91	0.00	0.00	-0.35	0.00	RB
incF	CTL0372	-1.11	0.00	0.00	-0.28	0.44	RB
incG	CTL0373	-1.04	-0.52	-0.90	-1.75	0.00	RB
CTL0375	CTL0375	0.00	0.00	0.00	0.00	2.46	RB
araD	CTL0376	-0.52	0.00	-0.68	-0.46	0.91	RB
efp_2	CTL0377	0.00	0.00	-0.46	-0.53	0.93	RB
accB	CTL0378	-0.28	0.47	-0.45	-0.42	1.06	RB
accC	CTL0379	-0.38	0.46	0.00	0.00	1.63	RB
rplM	CTL0380	-0.97	0.00	-0.52	-0.37	0.00	RB
rpsI	CTL0381	-0.82	0.22	-0.63	-0.51	0.20	RB
CTL0382	CTL0382	0.00	0.00	0.00	0.00	1.58	RB
CTL0388	CTL0388	-0.32	0.00	0.00	0.00	2.13	RB
CTL0389	CTL0389	-1.98	0.00	0.00	0.69	0.86	RB
garD (incU)	CTL0390	-1.67	0.32	0.00	0.00	0.54	RB
CTL0391	CTL0391	0.00	0.00	-0.57	0.00	-0.91	RB
CTL0392	CTL0392	0.36	-0.40	0.00	0.00	-0.80	RB
CTL0393	CTL0393	0.38	-0.40	-0.79	0.00	-1.13	RB
oppA	CTL0394	0.00	0.00	-0.90	-1.05	-0.77	RB
CTL0395	CTL0395	0.00	-0.83	0.00	0.00	-0.77	RB
CTL0396	CTL0396	0.00	-0.59	0.00	-0.42	-1.37	RB
pkn1	CTL0400	0.15	0.00	-0.67	-0.35	-1.23	RB
incS	CTL0402	-0.55	0.00	0.42	1.03	0.00	RB
rpmG	CTL0405	-0.86	0.00	0.00	0.00	0.00	RB
CTL0406	CTL0406	-0.54	0.45	0.48	0.00	0.00	RB
CTL0408	CTL0408	0.00	1.00	0.00	-0.32	0.00	RB
CTL0414_(Pl	CTL0414	0.00	-0.74	0.63	0.00	-1.11	RB
CTL0414a	CTL0414a	0.00	0.00	0.00	0.00	-0.84	RB
CTL0419	CTL0419	-0.27	-0.30	-1.05	-0.72	-0.76	RB
CTL0420	CTL0420	-0.90	0.00	0.00	0.00	0.00	RB
CTL0421	CTL0421	-1.47	0.00	0.00	0.00	0.00	RB
trpR	CTL0422	-0.90	0.00	0.00	0.00	1.07	RB
CTL0422a	CTL0422a	-0.62	0.00	0.00	0.00	0.00	RB
trpB	CTL0423	-1.36	-0.79	1.16	0.92	0.00	RB
trpA	CTL0424	0.00	-0.66	0.00	-0.53	-1.25	RB
CTL0425	CTL0425	0.00	0.00	0.00	-0.54	-1.18	RB
oppA2	CTL0427	-0.50	0.00	0.00	-0.70	-0.45	RB
CTL0431	CTL0431	-1.10	-0.91	1.00	0.98	-1.25	RB
CTL0432	CTL0432	-0.94	0.00	1.35	1.44	-0.42	RB
kdsB	CTL0434	-0.90	0.00	0.85	0.34	-0.43	RB

pyrG	CTL0435	0.00	0.00	0.00	-0.80	-1.48	RB
zwf	CTL0437	-0.41	0.00	0.00	-0.36	-1.18	RB
devB	CTL0438	-0.34	0.00	0.00	0.00	-0.91	RB
tmk	CTL0440	-0.59	0.34	0.00	0.00	0.00	RB
gyrA	CTL0441	-0.27	0.36	0.00	0.00	-0.90	RB
gyrB_2	CTL0442	-0.25	0.35	0.00	0.00	-0.94	RB
CTL0443	CTL0443	-0.57	0.00	0.00	0.00	-1.59	RB
CTL0444	CTL0444	-1.58	0.00	1.38	0.71	0.89	RB
tgt	CTL0445	-0.90	0.52	0.00	0.00	0.54	RB
mgtE	CTL0446	-0.96	-0.48	0.00	0.47	0.00	RB
CTL0447	CTL0447	-0.66	0.63	-0.42	0.00	-0.62	RB
tsaD	CTL0449	-0.68	0.00	-0.66	-0.61	0.00	RB
oppB	CTL0451	0.00	0.00	-0.34	0.00	0.00	RB
oppC	CTL0452	-0.33	0.00	0.00	-0.47	-0.57	RB
leuS	CTL0461	-0.90	0.87	-0.30	0.31	1.05	RB
hemL	CTL0462	-0.21	-0.74	-0.79	-0.33	0.45	RB
rpiA	CTL0465	0.48	-0.67	-0.45	0.59	-1.61	RB
xasA	CTL0468	0.43	0.00	0.00	0.00	-0.40	RB
CTL0469	CTL0469	-1.14	0.00	0.67	0.70	0.55	RB
ubiA	CTL0471	0.44	0.00	0.00	-0.66	0.00	RB
CTL0472	CTL0472	0.00	0.00	0.00	0.00	0.60	RB
CTL0473	CTL0473	-0.57	0.00	-1.12	-1.40	-1.76	RB
CTL0477	CTL0477	0.00	0.00	0.00	0.00	0.77	RB
CTL0477a	CTL0477a	0.00	0.00	-0.79	0.00	0.00	RB
CTL0478	CTL0478	-0.30	-0.81	-0.76	0.00	0.00	RB
CTL0479	CTL0479	-1.34	0.00	0.00	0.00	0.00	RB
CTL0480	CTL0480	-1.55	0.00	0.00	0.82	2.23	RB
cpoS	CTL0481	-0.56	0.64	0.00	2.40	0.96	RB
CTL0483	CTL0483	-0.51	0.00	0.00	0.00	1.61	RB
incB	CTL0484	-1.19	0.52	0.00	-0.77	2.39	RB
incC	CTL0485	-1.43	0.73	0.32	0.00	1.17	RB
CTL0486	CTL0486	-0.80	0.82	0.52	0.00	1.21	RB
CTL0487	CTL0487	-0.44	0.00	0.00	0.00	2.57	RB
acpP	CTL0488	-0.43	0.00	0.00	0.29	1.49	RB
fabG	CTL0489	-0.21	0.00	-0.78	-0.61	0.57	RB
fabD	CTL0490	-0.67	0.00	-0.51	0.00	0.62	RB
fabH	CTL0491	-0.85	0.27	-0.27	0.00	0.68	RB
CTL0493	CTL0493	-0.20	0.34	-0.71	-0.31	0.96	RB
ompH	CTL0494	0.00	0.42	-0.74	-0.75	0.94	RB
lpxD	CTL0495	0.40	0.00	-0.59	-0.75	0.00	RB
CTL0496	CTL0496	0.00	0.00	-0.60	0.38	1.97	RB
pdhA	CTL0497	0.00	0.00	-0.79	-1.01	0.50	RB
pdhB	CTL0498	0.25	0.00	0.00	-0.76	0.88	RB
pdhC	CTL0499	0.35	0.00	-0.57	-0.83	0.75	RB
CTL0500A	CTL0500a	0.00	0.68	-0.85	-0.58	-1.05	RB
dnaA_1	CTL0501	0.00	0.00	0.28	0.00	0.00	RB
oxaA	CTL0503	-0.46	0.36	0.00	0.29	0.00	RB
CTL0507	CTL0507	0.00	0.00	0.00	-0.42	-0.81	RB
ybjN	CTL0512	0.18	0.60	0.00	-0.43	-0.66	RB

dnaQ_1	CTL0513	0.29	0.46	0.00	0.00	-0.56	RB
CTL0516	CTL0516	0.37	0.00	0.00	0.00	0.00	RB
amiA	CTL0520	-0.77	0.44	-0.65	0.49	0.00	RB
murE	CTL0521	-0.79	0.34	-1.86	0.56	0.36	RB
mraW	CTL0524	-0.26	0.50	-1.08	-0.59	-0.75	RB
dnaA_2	CTL0527	0.22	0.00	0.00	-0.49	-0.54	RB
CTL0529	CTL0529	-1.12	0.00	0.00	0.00	0.00	RB
gcsH	CTL0534	0.25	0.00	-1.12	-0.69	-1.07	RB
CTL0535	CTL0535	0.00	0.29	-0.83	0.00	-0.44	RB
CTL0536	CTL0536	-1.01	0.91	-0.44	0.00	0.00	RB
lplA_1	CTL0537	-1.40	0.68	0.00	0.00	0.92	RB
mnmA	CTL0539	-0.59	0.00	0.90	0.71	1.96	RB
ptsN_1	CTL0542	-0.95	0.33	-0.37	0.00	0.76	RB
ptsN_2	CTL0543	-1.09	0.00	0.00	0.44	0.43	RB
dut	CTL0544	-0.60	0.00	0.00	0.28	0.88	RB
accD	CTL0545	-0.49	-0.25	0.48	0.00	0.00	RB
sodM	CTL0546	-0.35	0.00	0.00	0.00	0.57	RB
CTL0548	CTL0548	-1.09	0.71	-0.63	0.33	0.00	RB
rnc	CTL0549	0.00	0.49	-0.61	0.00	1.25	RB
radA	CTL0550	-0.25	0.00	-0.63	-0.28	0.53	RB
pknD	CTL0553	-0.53	0.00	0.48	0.34	3.25	RB
valS	CTL0554	-1.08	0.40	0.61	0.45	3.05	RB
CTL0555	CTL0555	-0.92	0.00	0.69	0.00	1.84	RB
atpI	CTL0557	-0.67	0.59	0.72	0.40	1.52	RB
atpD	CTL0558	-0.49	0.67	0.62	0.00	1.76	RB
atpB	CTL0559	-0.65	0.71	0.54	0.00	1.27	RB
atpA	CTL0560	-1.06	0.82	0.71	0.00	1.51	RB
CTL0561	CTL0561	-0.52	0.47	0.00	-0.73	2.07	RB
atpE	CTL0562	-0.81	0.50	0.30	-0.54	2.32	RB
rpoC	CTL0566	-1.31	0.84	1.02	1.06	2.96	RB
rpoB	CTL0567	-1.41	0.88	1.26	1.06	3.08	RB
rplL	CTL0568	-1.33	0.89	1.42	0.47	2.73	RB
rplJ	CTL0569	-1.45	0.65	1.34	0.57	2.94	RB
rplA	CTL0570	-1.44	0.81	1.18	0.50	2.93	RB
rplK	CTL0571	-1.22	0.83	1.05	0.47	3.07	RB
nusG	CTL0572	-1.00	0.69	0.39	0.00	2.75	RB
tufA	CTL0574	-1.34	0.90	0.00	0.00	2.09	RB
infA	CTL0575	-1.59	0.72	1.31	0.75	2.66	RB
CTL0576	CTL0576	0.42	0.00	0.86	0.37	3.93	RB
CTL0577	CTL0577	-0.88	0.00	1.05	0.00	4.95	RB
CTL0579	CTL0579	0.00	0.00	0.00	0.00	6.33	RB
CTL0580	CTL0580	-1.18	0.00	0.00	0.00	3.35	RB
trpC	CTL0581	-0.69	0.67	0.00	0.44	1.56	RB
xseA	CTL0583	0.00	0.71	0.00	0.47	0.61	RB
xseB	CTL0583a	-0.55	0.00	0.00	0.00	0.00	RB
CTL0584	CTL0584	-0.74	0.00	0.00	0.00	0.00	RB
ispS	CTL0585	-0.77	0.39	0.00	0.26	0.36	RB
pykF	CTL0586	0.24	0.50	-0.37	0.00	0.00	RB
dnaX_2	CTL0588	0.35	0.24	-0.43	-0.58	0.00	RB

CTL0589	CTL0589	0.49	0.77	0.00	0.63	0.00	RB
ptsI	CTL0590	-0.82	0.00	-0.68	0.00	0.00	RB
ptsH	CTL0591	-0.95	0.00	-0.78	0.00	0.00	RB
comE	CTL0593	0.00	0.00	0.00	-0.44	1.42	RB
CTL0594	CTL0594	-0.40	0.44	0.28	0.46	1.22	RB
dnaJ	CTL0595	-1.36	0.45	0.35	0.33	1.04	RB
rpsU	CTL0596	-0.76	0.58	0.39	0.51	1.18	RB
CTL0597	CTL0597	0.00	0.00	0.00	1.23	0.76	RB
CTL0600	CTL0600	-0.90	0.00	-0.40	0.00	1.07	RB
CTL0602	CTL0602	-1.03	0.78	0.51	0.94	0.00	RB
CTL0603	CTL0603	-0.91	0.00	0.00	0.00	0.00	RB
CTL0605	CTL0605	0.30	0.00	-0.39	0.00	0.00	RB
secG	CTL0606	0.00	0.00	-0.39	-0.94	-0.67	RB
def	CTL0607	-0.55	0.00	0.54	0.00	0.00	RB
ksgA	CTL0608	-0.23	0.00	0.86	0.94	0.00	RB
CTL0609	CTL0609	-0.74	0.00	0.62	0.66	-0.73	RB
CTL0611A	CTL0611a	0.00	0.00	0.00	0.64	0.91	RB
CTL0612	CTL0612	0.42	-0.52	0.00	0.63	0.35	RB
bioY	CTL0613	-1.49	0.00	0.73	1.09	0.93	RB
CTL0614	CTL0614	-0.97	0.00	0.00	0.57	0.00	RB
dapA	CTL0615	-1.96	0.40	-0.29	1.12	-0.79	RB
lysC	CTL0616	-1.77	0.52	0.00	1.16	-0.51	RB
asd	CTL0617	-1.64	0.00	-0.40	0.49	0.00	RB
dapB	CTL0618	-1.99	0.00	0.00	0.68	0.00	RB
aroA	CTL0620	-0.50	0.74	0.00	0.00	0.00	RB
aroL	CTL0621	-0.48	0.00	-1.89	-1.33	-1.24	RB
aroC	CTL0622	-0.63	0.00	-1.06	-0.70	-0.59	RB
aroB	CTL0623	-0.74	0.00	0.00	0.60	0.00	RB
aroD	CTL0624	-0.62	0.00	0.00	0.00	-0.59	RB
CTL0625	CTL0625	-0.90	0.00	0.00	-0.38	0.00	RB
CTL0634	CTL0634	-0.63	0.26	0.00	0.35	-0.55	RB
phnP	CTL0635	-0.41	0.00	0.00	0.00	-0.63	RB
artJ	CTL0636	-0.31	0.25	-0.35	0.00	0.00	RB
CTL0639	CTL0639	-1.00	0.00	0.00	0.00	1.09	RB
CTL0641	CTL0641	0.00	0.00	0.00	-0.42	-1.04	RB
CTL0642	CTL0642	-0.29	0.00	0.00	0.00	-0.82	RB
CTL0644	CTL0644	-0.84	0.74	0.00	0.00	0.00	RB
dapL	CTL0646	-0.52	0.36	0.46	0.00	-0.39	RB
CTL0647	CTL0647	0.00	0.00	0.00	0.00	-1.19	RB
proS	CTL0649	-0.67	0.43	0.28	0.00	1.97	RB
grpE	CTL0651	0.27	-0.63	0.00	0.00	-0.45	RB
dnaK	CTL0652	0.00	-0.38	-0.82	0.00	-0.57	RB
vacB	CTL0654	-1.08	0.48	0.85	0.94	1.87	RB
CTL0655	CTL0655	-0.87	0.28	0.45	0.00	0.28	RB
gltT	CTL0658	-0.84	0.00	-0.35	0.00	-0.39	RB
lpxK	CTL0659	-1.16	0.00	0.49	0.94	0.00	RB
CTL0660	CTL0660	-1.18	0.00	0.00	0.75	0.00	RB
CTL0661	CTL0661	-1.50	0.00	0.00	0.75	0.00	RB
ribC	CTL0662	-1.68	0.00	0.00	1.38	1.16	RB

nrdR	CTL0663	-0.20	-0.53	-1.11	0.00	0.00	RB
CTL0666	CTL0666	-0.74	0.32	0.00	0.00	0.00	RB
pcnB_2	CTL0667	0.29	0.00	-0.74	-0.96	-0.65	RB
lpxB	CTL0668	0.39	0.00	-0.39	-0.79	-0.64	RB
pmpA	CTL0669	-1.88	0.42	-0.60	0.00	0.00	RB
CTL0672	CTL0672	-1.15	0.46	0.00	0.00	1.59	RB
CTL0673	CTL0673	-0.55	0.00	0.00	0.00	1.96	RB
CTL0674	CTL0674	-0.78	0.00	0.00	0.00	1.73	RB
obgE	CTL0675	-1.70	-0.87	0.00	0.00	0.90	RB
rpmA	CTL0676	-1.55	0.00	0.68	0.42	1.38	RB
rplU	CTL0677	-1.41	0.44	0.43	0.35	1.57	RB
CTL0679	CTL0679	-0.85	0.72	0.65	0.00	0.00	RB
CTL0680	CTL0680	-0.85	0.00	0.00	0.00	0.00	RB
CTL0681	CTL0681	-0.81	0.00	0.50	0.00	0.00	RB
CTL0684	CTL0684	0.00	-0.24	-0.94	-0.75	0.00	RB
CTL0685	CTL0685	0.24	0.00	-0.56	-0.51	1.10	RB
CTL0686	CTL0686	0.00	0.00	0.00	0.00	2.23	RB
CTL0688	CTL0688	-0.34	0.23	0.26	0.34	0.28	RB
dapF	CTL0689	0.00	0.00	-1.22	-0.37	0.00	RB
clpP_2	CTL0690	-0.27	0.00	-1.25	-0.25	-0.35	RB
glyA	CTL0691	0.19	0.63	-0.78	-0.63	0.00	RB
CTL0694	CTL0694	-1.19	0.69	1.18	0.76	1.99	RB
rpsJ	CTL0695	-0.77	0.73	0.54	0.38	0.97	RB
fusA	CTL0696	-1.23	0.61	1.13	0.69	1.09	RB
rpsG	CTL0697	-1.48	0.70	1.22	0.49	1.13	RB
rpsL	CTL0698	-1.40	0.67	1.08	0.35	0.93	RB
CTL0699	CTL0699	-1.06	0.00	0.00	0.00	1.98	RB
gltX	CTL0705	-0.72	0.59	0.79	0.56	1.39	RB
recJ	CTL0707	0.18	0.47	0.00	0.65	0.57	RB
secF	CTL0708a	-0.40	0.48	0.00	0.69	0.24	RB
CTL0709	CTL0709	-1.74	0.00	0.00	0.00	1.79	RB
uppS	CTL0710	-0.36	0.39	-0.57	-0.33	0.63	RB
cdsA	CTL0711	0.38	0.00	0.00	-0.43	0.00	RB
cmk	CTL0712	0.00	0.00	0.00	-0.33	0.00	RB
plsC	CTL0713	0.00	0.31	0.00	0.00	0.00	RB
argS	CTL0714	-0.27	0.36	0.00	0.00	0.74	RB
murA	CTL0715	0.00	0.48	0.00	0.46	0.88	RB
yepC	CTL0717	-0.89	0.29	0.34	0.66	0.00	RB
prfB	CTL0719	-0.46	0.00	0.35	0.30	0.00	RB
CTL0720	CTL0720	0.32	0.00	0.00	-0.65	-0.90	RB
CTL0721	CTL0721	0.32	0.00	0.00	-0.27	-0.58	RB
truA	CTL0723	0.00	-0.38	0.00	0.00	-0.69	RB
CTL0729	CTL0729	0.00	0.00	0.00	0.00	1.03	RB
CTL0733	CTL0733	-0.44	0.50	-0.81	-0.71	0.38	RB
CTL0735	CTL0735	0.00	0.56	0.00	0.00	0.00	RB
pheT	CTL0736	-0.44	0.84	0.00	0.00	1.03	RB
oppC2	CTL0739	0.00	0.00	-0.34	0.55	0.00	RB
oppB2	CTL0740	0.00	0.00	-0.40	0.41	0.55	RB
oppA4	CTL0741	0.00	0.00	-0.64	0.00	0.00	RB

CTL0744	CTL0744	0.00	0.00	0.00	0.00	2.69	RB
CTL0748	CTL0748	0.00	0.00	0.00	-0.47	0.45	RB
rho	CTL0752	-0.41	-0.49	0.47	1.32	1.24	RB
coaE	CTL0753	-0.29	-0.47	0.88	1.68	1.83	RB
polA	CTL0754	0.36	-0.57	0.71	2.28	1.12	RB
sohB	CTL0755	0.30	-0.63	0.75	2.25	0.84	RB
CTL0756	CTL0756	-0.62	0.26	0.29	-0.35	0.24	RB
pgsA_2	CTL0757	0.00	-0.27	0.00	0.00	0.82	RB
dnaB	CTL0759	0.40	0.30	-0.63	0.00	2.47	RB
gidA	CTL0760	-1.31	0.69	1.27	0.84	2.55	RB
lplA_2	CTL0761	-0.71	-0.67	0.00	0.00	1.63	RB
ndk	CTL0762	-0.58	0.00	0.00	0.54	1.52	RB
grgA	CTL0766	-0.47	0.21	0.52	0.47	1.88	RB
gapA	CTL0767	-0.62	0.00	0.52	0.31	1.68	RB
rplQ	CTL0768	-1.22	0.93	0.98	0.80	2.14	RB
rpoA	CTL0769	-1.30	0.81	1.08	0.75	2.09	RB
rpsK	CTL0770	-1.23	0.82	0.93	0.46	1.76	RB
rpsM	CTL0771	-1.29	0.55	1.00	0.70	2.23	RB
secY	CTL0772	-1.38	0.62	0.47	0.56	2.11	RB
rplO	CTL0773	-2.02	0.86	0.82	0.60	2.37	RB
rpsE	CTL0774	-2.01	0.94	0.95	0.73	2.42	RB
rplR	CTL0775	-1.66	0.62	0.85	0.69	2.73	RB
rplF	CTL0776	-1.81	0.75	1.22	0.96	2.74	RB
rpsH	CTL0777	-1.77	0.74	1.21	0.90	3.07	RB
rplE	CTL0778	-1.76	0.61	1.19	0.97	2.78	RB
rplX	CTL0779	-2.05	0.72	1.09	0.88	3.16	RB
rplN	CTL0780	-2.12	0.64	1.26	1.04	2.99	RB
rpsQ	CTL0781	-2.05	0.80	1.15	0.87	3.17	RB
rplP	CTL0783	-2.36	0.93	1.37	1.05	3.48	RB
rpsC	CTL0784	-2.32	0.93	1.24	1.01	3.54	RB
rplV	CTL0785	-1.77	0.86	1.26	1.11	3.50	RB
rpsS	CTL0786	-1.90	0.43	1.36	0.98	3.03	RB
rplB	CTL0787	-1.94	0.92	1.38	1.20	3.34	RB
rplD	CTL0789	-1.87	0.74	1.32	1.00	3.10	RB
rplC	CTL0790	-1.20	0.69	1.13	0.79	2.82	RB
Cap1	CTL0791	-0.31	0.87	-2.16	-0.74	1.46	RB
fmt	CTL0792	-0.39	0.00	0.50	0.65	1.64	RB
lpxA	CTL0793	0.00	0.00	0.00	0.00	0.79	RB
lpxC	CTL0795	0.23	0.00	0.00	0.00	0.26	RB
dnaQ_2	CTL0798	0.00	0.00	0.42	0.53	3.30	RB
CTL0799	CTL0799	0.42	0.00	0.84	0.85	3.15	RB
CTL0800	CTL0800	-0.74	0.00	0.00	0.38	2.66	RB
trxA	CTL0801	-0.43	0.37	-0.98	-0.49	1.72	RB
CTL0802	CTL0802	-0.41	0.00	0.00	0.96	2.55	RB
mip	CTL0803	0.00	0.00	-0.88	0.00	1.13	RB
aspS	CTL0804	-0.72	0.28	-0.59	0.30	1.26	RB
hisS	CTL0805	-0.70	0.28	-0.37	0.46	1.81	RB
uhpC	CTL0806	0.00	0.00	0.56	0.00	0.00	RB
dnaE	CTL0807	0.00	0.00	0.89	0.68	1.29	RB

CTL0809	CTL0809	0.24	0.00	-0.92	-0.47	0.00	RB
CTL0810	CTL0810	0.42	0.00	0.00	0.00	0.86	RB
rsbW	CTL0811	0.00	0.00	0.00	0.39	0.00	RB
dacC	CTL0813	0.40	0.00	0.00	0.00	0.00	RB
CTL0814	CTL0814	-0.49	0.96	-1.50	-1.10	0.00	RB
brnQ	CTL0817	-0.49	0.00	-0.55	0.00	-0.42	RB
CTL0818	CTL0818	-0.52	0.36	0.29	0.71	1.01	RB
lpdA	CTL0820	0.39	0.34	-0.81	0.00	0.00	RB
CTL0829	CTL0829	0.00	0.00	0.00	0.72	-0.52	RB
CTL0830	CTL0830	-0.74	0.00	0.00	0.88	0.00	RB
CTL0831	CTL0831	-1.05	0.00	0.00	1.10	0.00	RB
gspG	CTL0832	-0.82	-0.41	0.00	0.75	0.00	RB
gspF	CTL0833	-0.91	0.00	0.43	1.67	0.00	RB
gspE	CTL0834	-0.89	0.00	0.57	1.72	0.56	RB
gspD	CTL0835	-1.27	0.00	0.95	2.17	1.62	RB
CTL0836	CTL0836	-1.67	-0.49	0.77	1.76	1.80	RB
pepP	CTL0837	0.00	0.64	-0.53	0.46	0.00	RB
CTL0843	CTL0843	-1.05	0.00	-0.46	0.45	-0.59	RB
thrS	CTL0844	-0.67	0.81	-0.74	0.71	0.32	RB
minD	CTL0845	0.00	0.00	-0.45	0.00	-0.98	RB
pGP6-D-rela	CTL0846	-0.20	0.00	-0.52	0.00	-1.00	RB
CTL0847	CTL0847	0.00	0.49	-0.74	0.00	-1.46	RB
trpS	CTL0848	-0.42	0.56	-0.53	0.00	-0.77	RB
uvrB	CTL0849	0.00	0.75	0.00	0.00	-0.74	RB
eno	CTL0850	0.28	0.00	-1.13	-0.68	-1.58	RB
tatD	CTL0858	0.00	0.39	0.30	0.00	0.00	RB
tolB	CTL0862	0.22	0.50	-0.84	-0.44	-0.55	RB
CTL0869	CTL0869	-0.49	0.00	0.00	0.00	0.00	RB
ung	CTL0871	0.00	0.75	0.00	0.00	0.00	RB
uvrD	CTL0872	-0.57	0.27	0.00	0.00	-0.88	RB
CTL0874	CTL0874	-0.86	0.31	0.00	-0.46	-0.93	RB
CTL0875	CTL0875	-1.04	0.56	0.52	0.00	0.00	RB
folA	CTL0876	-1.64	0.95	1.48	1.09	0.78	RB
folP	CTL0877	-1.94	0.57	1.06	0.60	0.00	RB
folX	CTL0878	-0.62	0.00	0.00	0.63	0.00	RB
rpoD	CTL0879	-0.39	0.30	-0.52	0.00	-0.36	RB
rpsT	CTL0881	-1.24	0.48	0.65	1.02	0.95	RB
CTL0887	CTL0887	-1.64	-0.55	-0.35	0.41	-0.64	RB
mviN	CTL0888	-0.43	0.61	0.00	0.73	0.98	RB
nfo	CTL0889	0.20	0.43	0.00	0.00	0.64	RB
rpsD	CTL0890	-1.33	0.62	0.80	0.34	0.98	RB
CTL0891	CTL0891	-0.84	0.00	0.00	0.00	0.82	RB
ispA	CTL0892	0.00	-0.45	0.00	-0.42	-0.53	RB
CTL0895	CTL0895	-1.70	0.00	0.37	0.00	0.70	RB
CTL0897	CTL0897	0.46	0.00	0.00	0.00	0.00	RB
CTL0010	CTL0010	2.22	-0.47	-0.58	-0.40	-0.61	IB
CTL0028	CTL0028	3.20	-1.06	0.62	0.00	-1.85	IB
aspC_2	CTL0044	3.87	0.00	0.49	0.00	-0.73	IB
pgk	CTL0062	2.00	-0.56	-0.48	-0.75	-0.36	IB

CTL0065	CTL0065	1.78	0.00	0.00	0.67	0.00	IB
porB	CTL0082	3.64	-0.83	0.00	-0.99	-2.74	IB
fliI	CTL0086	5.37	-0.88	0.00	-1.59	-1.44	IB
CTL0087	CTL0087	4.86	-0.99	0.00	-2.70	-2.93	IB
fliF	CTL0088	3.11	-1.49	1.10	0.00	-0.55	IB
hctA	CTL0112	7.27	-0.59	1.63	-1.43	-2.04	IB
rbsV	CTL0134	1.56	0.00	-1.56	-0.69	0.00	IB
CTL0148	CTL0148	1.94	-0.40	-1.00	-1.50	-1.06	IB
CTL0149	CTL0149	2.33	-0.89	0.00	-0.89	-1.92	IB
CTL0152	CTL0152	3.06	-1.45	-0.56	-1.09	-1.51	IB
CTL0173a	CTL0173a	3.80	0.69	-1.23	-0.95	0.00	IB
CTL0174	CTL0174	1.70	0.00	0.00	-0.74	1.61	IB
sucC	CTL0193	4.23	-0.82	0.00	-0.90	-2.48	IB
sucD	CTL0194	3.71	-1.03	0.00	-1.11	-2.23	IB
CTL0228	CTL0228	2.45	-0.65	0.00	-0.59	-1.74	IB
pmpE	CTL0248	3.52	-0.74	0.65	-0.67	-2.58	IB
pmpF	CTL0249	3.74	-0.61	0.47	-0.93	-2.64	IB
pmpG	CTL0250	3.12	-0.83	0.52	-0.36	-2.40	IB
pmpH	CTL0251	2.99	-0.77	0.56	-0.40	-2.20	IB
CTL0256	CTL0256	3.29	-0.72	0.00	-1.52	-1.83	IB
CTL0276	CTL0276	1.76	0.00	-0.72	-0.68	0.00	IB
sucA	CTL0310	4.03	-1.63	0.00	-1.21	-2.80	IB
sucB_1	CTL0311	3.91	-1.72	0.00	-1.46	-2.63	IB
flhA	CTL0316	4.37	-1.31	0.00	-1.92	-2.60	IB
CTL0339_(PL	CTL0339	4.33	-1.72	0.00	1.98	-1.92	IB
malQ	CTL0342	4.21	-1.11	0.35	-1.10	-2.08	IB
scc1	CTL0343	4.69	-1.07	0.00	-1.07	-2.41	IB
copN	CTL0344	3.90	-0.89	0.00	-1.44	-2.62	IB
lcrD	CTL0345	2.35	-0.86	0.00	-1.06	-2.11	IB
dsbB	CTL0428	4.16	0.00	0.00	-1.15	-1.79	IB
dsbG	CTL0429	3.63	-0.41	0.38	-1.18	-2.35	IB
CTL0430	CTL0430	3.96	-1.01	0.00	-0.75	-1.48	IB
CTL0464	CTL0464	2.57	-0.57	0.00	-0.45	-2.19	IB
glgP	CTL0500	3.17	-1.30	0.59	-0.38	-1.39	IB
CTL0511	CTL0511	1.37	0.00	0.54	0.00	-0.63	IB
HU	CTL0519	2.97	-0.74	0.00	-0.94	-1.39	IB
CTL0525	CTL0525	2.40	-0.55	-0.59	-1.48	-1.83	IB
clpC	CTL0538	1.90	0.66	0.42	0.00	-1.13	IB
CTL0541	CTL0541	1.96	-1.02	-0.24	-0.88	-0.87	IB
CTL0626	CTL0626	3.90	-0.75	0.00	-1.08	-2.84	IB
CTL0627	CTL0627	4.31	-1.12	1.18	-1.02	-3.47	IB
CTL0628	CTL0628	3.43	-0.98	1.04	-0.90	-2.31	IB
CTL0645	CTL0645	3.03	-0.59	-0.47	-1.31	-2.47	IB
pmpB	CTL0670	3.99	-0.28	0.00	-0.72	-2.43	IB
pmpC	CTL0671	2.04	0.00	-1.43	0.00	-1.56	IB
rsbV	CTL0683	3.46	-1.05	-0.51	-1.70	-1.98	IB
ctcB	CTL0727	4.11	-1.16	-0.37	5.22	-1.84	IB
ctcC	CTL0728	4.53	-1.46	0.00	-1.11	-1.55	IB
sctL	CTL0824	2.64	-0.85	-0.30	-1.07	-1.27	IB

CTL0824a	CTL0824a	2.61	-0.65	0.00	-0.83	-1.01	IB
sctR	CTL0825	2.65	-0.68	0.00	-1.09	-1.25	IB
sctT	CTL0827	2.39	-0.60	0.30	-0.71	-1.10	IB
CTL0828	CTL0828	3.80	-1.88	0.00	0.35	-2.85	IB
rsbU	CTL0851	2.21	0.00	0.00	-0.73	-1.39	IB
CTL0852	CTL0852	3.53	-0.65	0.00	-1.00	-1.54	IB
CTL0853	CTL0853	3.91	-0.76	0.27	-1.03	-2.33	IB
CTL0865	CTL0865	2.92	-0.38	0.49	-0.59	-1.82	IB
groEL2	CTL0867	3.11	-0.49	-0.39	-0.61	-1.99	IB
CTL0870	CTL0870	2.82	-1.44	0.00	-1.16	-2.37	IB
CTL0885	CTL0885	4.97	-1.78	0.27	-1.24	-2.12	IB
chxR	CTL0894	4.25	-1.44	0.28	-1.51	-2.67	IB
scc5	CTL0003	2.90	-1.59	1.81	2.95	-1.66	EB
CTL0052	CTL0052	1.94	-1.81	1.46	1.44	-1.74	EB
tmeA	CTL0063	4.22	-2.05	2.05	2.66	-1.56	EB
tmeB	CTL0064	2.16	-1.78	1.92	2.43	-1.59	EB
CTL0080	CTL0080	3.12	-2.31	2.23	2.85	-0.35	EB
CTL0081	CTL0081	4.54	-2.06	1.99	2.41	-1.15	EB
glgA	CTL0167	6.87	-2.11	1.07	1.65	-2.86	EB
CTL0185	CTL0185	5.81	-1.42	1.82	3.18	-3.08	EB
CTL0186	CTL0186	4.96	-1.81	2.41	3.70	-2.55	EB
CTL0209	CTL0209	2.14	-1.80	2.14	2.71	0.00	EB
CTL0219	CTL0219	5.65	-2.18	1.97	2.71	-1.97	EB
CTL0220	CTL0220	5.97	-1.92	2.01	2.72	-2.06	EB
CTL0221	CTL0221	5.76	-2.09	2.23	3.07	-2.18	EB
tepP	CTL0255	5.51	-1.89	2.73	4.24	-2.63	EB
incV	CTL0260	1.55	-1.13	1.89	3.18	-1.75	EB
hctB	CTL0302	6.60	-1.53	2.88	3.26	2.33	EB
CTL0329	CTL0329	6.79	-1.98	2.82	3.40	-1.44	EB
ltuB	CTL0336	4.84	-2.30	2.39	3.44	-2.12	EB
CTL0337	CTL0337	2.61	-1.52	3.26	3.85	-2.52	EB
CTL0338	CTL0338	3.77	-1.73	3.00	4.39	-2.90	EB
CTL0338A	CTL0338a	4.06	-2.28	2.45	3.91	-4.65	EB
CTL0386	CTL0386	3.60	-1.58	1.24	1.24	-0.81	EB
CTL0433	CTL0433	4.59	-1.66	2.60	3.35	-3.03	EB
CTL0540	CTL0540	2.08	-1.01	2.08	3.10	-0.58	EB
CTL0610	CTL0610	3.25	-2.25	2.12	3.61	-1.79	EB
CTL0619	CTL0619	2.60	-1.48	1.17	2.47	-1.93	EB
CTL0638	CTL0638	4.99	-1.35	1.38	2.20	-1.34	EB
CTL0648	CTL0648	5.32	-2.19	1.98	3.21	-2.36	EB
tsp	CTL0700	4.76	-1.51	2.54	2.03	-1.39	EB
omcB	CTL0702	4.71	-2.14	2.58	3.63	-2.92	EB
omcA	CTL0703	5.91	-1.52	2.70	4.08	-3.06	EB
CTL0704	CTL0704	4.53	-0.74	1.05	1.84	0.00	EB
tarp	CTL0716	6.23	-2.19	2.86	3.98	-2.47	EB
glgC	CTL0750	2.84	-1.99	1.97	2.18	-0.86	EB
CTL0808	CTL0808	4.30	-1.95	1.67	2.32	-1.62	EB
scc2	CTL0839	5.84	-1.82	2.45	4.68	-2.91	EB
CTL0840	CTL0840	6.42	-1.94	2.53	4.49	-2.72	EB

copB	CTL0841	5.15	-2.23	2.95	5.12	-3.06	EB
copD	CTL0842	5.55	-1.89	2.72	4.97	-3.30	EB
CTL0883	CTL0883	4.76	-1.81	2.33	4.56	-1.92	EB
CTL0884	CTL0884	5.24	-1.95	1.73	3.69	-1.87	EB
CTL0886	CTL0886	3.62	-1.53	2.16	3.83	-2.44	EB

Table S2 Type III operons

First Gene							
cdsE	cdsF	cdsG	CTL0037	sctN	cdsO	CTL0040	sctQ
sctU	sctV	lcrD	copN	scc1	malQ		
scc2	CTL0840	copB_1	copD_1				
CTL0238	scc3	copB_2	copD_2				
sctL	sctR	sctS	sctT				
sctJ	sctK						
fliI	CTL0085						
scc4	cdsD						
fliF							
flhA							
cdsC							

Table S3 T3SS Efector Genes

gene_num	gene_name	18hpi vs 24hpi	euo 24h vs clover 24h	hctA 18h vs clover 18h	ctcB_18h vs clover 18h	hctB_24h vs clover 24h
CTL0063	tmeA	4.22	-2.05	2.05	2.66	-1.56
CTL0064	tmeB	2.16	-1.78	1.92	2.43	-1.59
CTL0080	CTL0080	3.12	-2.31	2.23	2.85	-0.35
CTL0081	CTL0081	4.54	-2.06	1.99	2.41	-1.15
CTL0219	CTL0219	5.65	-2.18	1.97	2.71	-1.97
CTL0220	CTL0220	5.97	-1.92	2.01	2.72	-2.06
CTL0221	CTL0221	5.76	-2.09	2.23	3.07	-2.18
CTL0255	tepP	5.51	-1.89	2.73	4.24	-2.63
CTL0338	CTL0338	3.77	-1.73	3.00	4.39	-2.90
CTL0338a	CTL0338A	4.06	-2.28	2.45	3.91	-4.65
CTL0360	cteG	1.19	2.26	0.00	0.69	1.25
CTL0397	CTL0397	4.81	-1.76	0.99	1.82	-2.84
CTL0398	CTL0398	5.46	-1.41	0.98	1.77	-2.48
CTL0399	CTL0399	4.13	-1.26	0.79	1.55	-1.97
CTL0417	CTL0417	1.17	0.00	0.00	0.00	0.00
CTL0419	CTL0419	-0.27	-0.30	-1.05	-0.72	-0.76
CTL0716	tarp	6.23	-2.19	2.86	3.98	-2.47
CTL0812	CTL0812	2.18	-0.84	0.47	0.33	-0.44
CTL0870	CTL0870	2.82	-1.44	0.00	-1.16	-2.37
CTL0883	CTL0883	4.76	-1.81	2.33	4.56	-1.92
CTL0884	CTL0884	5.24	-1.95	1.73	3.69	-1.87
CTL0885	CTL0885	4.97	-1.78	0.27	-1.24	-2.12
CTL0886	CTL0886	3.62	-1.53	2.16	3.83	-2.44

Table S4 Inc Protein Genes

gene_num	gene_name	18hpi vs 24hpi	euo 24h vs clover 24h	hctA 18h vs clover 18h	ctcB_18h vs clover 18h	hctB_24h vs clover 24h
CTL0184	InaC	-0.30	-0.33	-0.60	0.72	-0.37
CTL0223	CTL0223	-0.17	0.00	0.00	-0.37	-1.43
CTL0260	incV	1.55	-1.13	1.89	3.18	-1.75
CTL0261	CTL0261	-1.50	0.00	0.00	0.00	0.54
CTL0356	mrcA	-0.88	0.49	0.00	0.00	0.91
CTL0370	incD	-1.05	-0.56	0.00	0.00	0.30
CTL0371	incE	-0.91	0.00	0.00	-0.35	0.00
CTL0372	incF	-1.11	0.00	0.00	-0.28	0.44
CTL0373	incG	-1.04	-0.52	-0.90	-1.75	0.00
CTL0374	incA	2.35	1.25	-2.83	-0.93	2.34
CTL0389	CTL0389	-1.98	0.00	0.00	0.69	0.86
CTL0390	garD (incU)	-1.67	0.32	0.00	0.00	0.54
CTL0402	incS	-0.55	0.00	0.42	1.03	0.00
CTL0431	CTL0431	-1.10	-0.91	1.00	0.98	-1.25
CTL0444	CTL0444	-1.58	0.00	1.38	0.71	0.89
CTL0448	CTL0448	0.00	0.00	0.00	0.00	0.00
CTL0466	CTL0466	1.68	-1.20	0.49	1.78	-2.20
CTL0475	CTL0475	0.00	-2.13	-3.69	0.57	0.00
CTL0476	iPAM	0.00	-3.36	-4.50	0.23	0.40
CTL0477	CTL0477	0.00	0.00	0.00	0.00	0.77
CTL0477a	CTL0477a	0.00	0.00	-0.79	0.00	0.00
CTL0478	CTL0478	-0.30	-0.81	-0.76	0.00	0.00
CTL0479	CTL0479	-1.34	0.00	0.00	0.00	0.00
CTL0480	CTL0480	-1.55	0.00	0.00	0.82	2.23
CTL0481	cpoS	-0.56	0.64	0.00	2.40	0.96
CTL0484	incB	-1.19	0.52	0.00	-0.77	2.39
CTL0485	incC	-1.43	0.73	0.32	0.00	1.17
CTL0486	CTL0486	-0.80	0.82	0.52	0.00	1.21
CTL0540	incM	2.08	-1.01	2.08	3.10	-0.58
CTL0599	CTL0599	1.46	0.00	-2.72	-1.62	0.00
CTL0611a	CTL0611A	0.00	0.00	0.00	0.64	0.91
CTL0612	CTL0612	0.42	-0.52	0.00	0.63	0.35
CTL0639	CTL0639	-1.00	0.00	0.00	0.00	1.09
CTL0709	CTL0709	-1.74	0.00	0.00	0.00	1.79
CTL0744	CTL0744	0.00	0.00	0.00	0.00	2.69
CTL0791	Cap1	-0.31	0.87	-2.16	-0.74	1.46
CTL0882	CTL0882	-0.75	-1.07	0.00	0.46	0.00

Table S5 Primers

Construct	Sequence	Primer name	Template
E-hctA	ttttagcgcgctcaccatcttgttgttacctccttagc	3’ hctA bb	E-clover (Grieshaber et al., 2022)
	aacaaaaaaaatggactacaaagaccatgacggtgattataaagatcatg	5' hctA bb	
	gatggtgagcgcgctaaaagatacggcaaaaaaaatgactgacttgttgg	5’ hctA i	L2 genomic
	tgtagtccattttttttgttgagcgagtttttttcgctgttttaactttgttttagg	3' hctA i	
E-euo	ttttatctcaatggactacaaagaccatgacggtgattataaagatcatg	5' euo bb	E-clover (Grieshaber et al., 2022)
	gtaagcattcgctcaccatcttgttgttacctccttagcagggt	3' euo bb	
	gatggtgagcgaatgcttacaacaagatacaggggtcgaagcagaac	5' euo i	L2 genomic
	TGTAGTCcattgagataaaattttctgcgtctgccagcaaatctgc	3' euo i	
E-ctcB	gactcctgctatggactacaaagaccatgacggtgattataaagatcatg	5' ctcB bb	E-clover (Grieshaber et al., 2022)
	atttttggcatcttgttgttacctccttagcagggtgctgc	3' ctcB bb	
	taacaacaagatgccaaaaatcgacacttgtgattcttgcgtttcc	5' ctcB i	L2 genomic
	tgtagtccatagcaggagtccataggatggtaaaggtagtacg	3' ctcB i	
Bscieng	aaaagaaacgcgaattcggcatggtatcaaaaggtgaagccgtcatcaaag aatttatgagatttaaggtgcatatggagggtagtatgaacgggcacgagtttg agattgagggtgaaggcgaagggcgcccctacgaagggactcagaccgc taaattaaaagttactaaaggcggcccccttcccttctcctgggacatcttatct cctcaattcatgtacggctctcgtgccttcatcaaacaccccgcggacatccc cgattattacaagcagagttttccagagggttttaaatgggagcgtgttatgaat tttgaggatgggggagcggtgacagtaacacaggacacgtcacttgaggat ggtacattgatctacaaggtaaaattgcgaggtacaaactttccacctgacgg accagtcatgcaaaagaaaaccatgggctgggaggccagtacggaacgat tgtaccctgaggacggagtgttaaagggggatataaagatggcactacgtct aaaggatggagggcgatacttagcagacttcaaaacgacttacaaagcgaa gaagcctgttcaaatgcctggcgcgtataacgtggaccgcaaattagatata acttctcacaatgaagattacacagtagtcgagcagtatgagcgaagtgaag gcagacattccacaggaggaatggatgagctttacaaatagggatgacatgt gattcg	mScarlet I gBlock	
	tagggatgacatgtgattcgcgtaggaaaaagaggagggagacc	5’ sci bb	Bmelva (Chiarelli et al., 2023)
	gccgaattcgcgtttcttttgtactcccaacatgttcattcc	3' bsci bb	
	actgtataaataggacggatcccttgtacaatcaatttaccgattaaatagtctc	5' LVA delete bb	Bscielva
	atccgtcctatttatacagttcatccatgcccatcacatcgg	3' LVA delete bb	
Ascieng	caaaaaaaatggcggatccgatggtatcaaaaggtgaag	5' hctAsci bb	Bscieng
	tagaatctaaatgtaatacggttatccacagaatcaggggataacgc	3' hctAsci bb	
	cgtattacatttagattctagaaaatggttgcatgaatttgaacaaacaaac	5' hctAprom i	L2 genomic
	tcggatccgccattttttttgccgtatcttttagcgccatgaaaaaatatcc	3' hctAprom i	
Pscieng	ctatctccgtatggtatcaaaaggtgaagccgtcatcaaagaatttatg	5’ porBpscie bb	Bscieng
	agaaccttatatgtaatacggttatccacagaatcaggggataacgc	3' porBpsci bb	
	cgtattacatataaggttcttcttcaatgagaaaagactaaaacgccttcc	5' porBprom i	L2 genomic
	gactaaatgagtagcaagctagtgaactatctccgtatggtatcaa	3’ porBprom i	

Table S6 FISH probes

FISH Probes	L2 (LGV Bu434) location	Strand
euo	203142..203880	reverse
hctA	895571..896131	reverse
hctB	373642..374409	forward
porB	933057..934193	reverse
scc2-copD operon	967206..968729	forward
CTL0238-copD2 operon	741359..743881	reverse
sctL-sctR operon	952095..953717	forward
sctU-lcrD operon	609950..612290	reverse
incD-incG operon	457415..459091	forward
incV	710380..711498	reverse